

# Journal of Visualized Experiments

## Strategy for visualization, quantification, and mapping of immune cell populations in the tumor microenvironment --Manuscript Draft--

Article Type:	Invited Methods Article - JoVE Produced Video
Manuscript Number:	JoVE60740R2
Full Title:	Strategy for visualization, quantification, and mapping of immune cell populations in the tumor microenvironment
Section/Category:	JoVE Immunology and Infection
Keywords:	tumor microenvironment; Multiplex Immunofluorescence; FFPE; image analysis; Tissue Alignment; Tissue Heat Map; VIS Software
Corresponding Author:	Naglaa Shoukry Centre de recherche du CHUM Montreal, Quebec CANADA
Corresponding Author's Institution:	Centre de recherche du CHUM
Corresponding Author E-Mail:	naglaa.shoukry@umontreal.ca
Order of Authors:	Manuel Flores Molina Thomas Fabre Aur�lie Cleret-Buhot Genevi�ve Soucy Liliane Meunier Mohamed N Abdelnabi Nicolas Belforte Simon Turcotte Naglaa Shoukry
Additional Information:	
Question	Response
Please indicate whether this article will be Standard Access or Open Access.	Open Access (US\$4,200)
Please indicate the <b>city, state/province, and country</b> where this article will be <b>filmed</b> . Please do not use abbreviations.	Montreal, QC, Canada

**TITLE:**

**Visualization, Quantification, and Mapping of Immune Cell Populations in the Tumor Microenvironment**

**AUTHORS:**

Manuel Flores Molina<sup>1,2</sup>, Thomas Fabre<sup>1,2\*</sup>, Aurélie Cleret-Buhot<sup>1</sup>, Geneviève Soucy<sup>1,3</sup>, Liliane Meunier<sup>1,4</sup>, Mohamed N. Abdelnabi<sup>1,2</sup>, Nicolas Belforte<sup>1,4</sup>, Simon Turcotte<sup>1,4,6</sup>, Naglaa H. Shoukry<sup>1,4,7</sup>

<sup>1</sup>Centre de Recherche du Centre hospitalier de l'Université de Montréal (CRCHUM), Montréal, Québec, Canada

<sup>2</sup>Département de Microbiologie, Infectiologie et Immunologie, Faculté de Médecine, Université de Montréal, Montréal, Québec, Canada

<sup>3</sup>Département de Pathologie et Biologie Cellulaire, Faculté de Médecine, Université de Montréal, Montréal, Québec, Canada

<sup>4</sup>Institut du Cancer de Montréal, Montréal, Québec, Canada

<sup>5</sup>Département de Neurosciences, Faculté de Médecine, Université de Montréal, Montréal, Québec, Canada

<sup>6</sup>Département de Chirurgie, Faculté de Médecine, Université de Montréal, Montréal, Québec, Canada

<sup>7</sup>Département de Médecine, Faculté de médecine, Université de Montréal, Montréal, Québec, Canada

\*Present affiliation: Pfizer Inc., Cambridge, MA, USA

**Corresponding Author:**

Naglaa H. Shoukry (naglaa.shoukry@umontreal.ca)

**KEYWORDS:**

tumor microenvironment, multiplex immunofluorescence, FFPE, image analysis, tissue alignment, tissue heat map, VIS software

**SUMMARY:**

Here, we describe a simple and accessible strategy for visualizing, quantifying, and mapping immune cells in formalin-fixed paraffin-embedded tumor tissue sections. This methodology combines existing imaging and digital analysis techniques with the purpose of expanding the multiplexing capability and multiparameter analysis of imaging assays.

**ABSTRACT:**

The immune landscape of the tumor microenvironment (TME) is a determining factor in cancer progression and response to therapy. Specifically, the density and the location of immune cells in the TME have important diagnostic and prognostic values. Multiomic profiling of the TME has exponentially increased our understanding of the numerous cellular and molecular networks regulating tumor initiation and progression. However, these techniques do not provide

information about the spatial organization of cells or cell-cell interactions. Affordable, accessible, and easy to execute multiplexing techniques that allow spatial resolution of immune cells in tissue sections are needed to complement single cell-based high-throughput technologies. Here, we describe a strategy that integrates serial imaging, sequential labeling, and image alignment to generate virtual multiparameter slides of whole tissue sections. Virtual slides are subsequently analyzed in an automated fashion using user-defined protocols that enable identification, quantification, and mapping of cell populations of interest. The image analysis is done, in this case using the analysis modules Tissuealign, Author, and HISTOmap. We present an example where we applied this strategy successfully to one clinical specimen, maximizing the information that can be obtained from limited tissue samples and providing an unbiased view of the TME in the entire tissue section.

## INTRODUCTION:

Cancer development is the result of a multistep process involving reciprocal interactions between malignant cells and the TME. Other than tumor cells, the TME is composed of nonmalignant cells, stromal cells, immune cell populations, and extracellular matrix (ECM)<sup>1</sup>. The spatial organization of the different cellular and structural components of the tumor tissue and the dynamic exchange between the cancer and neighboring non-cancer cells ultimately modulate tumor progression and response to therapy<sup>2-4</sup>. It has been shown that the immune response in cancer is spatiotemporally regulated<sup>5,6</sup>. Different immune cell populations infiltrating the neoplastic lesion and the adjacent tissue exhibit distinctive spatial distribution patterns and varied activation and differentiation states associated with different functions (e.g., pro- versus antitumor). These different immune populations and their parameters coevolve overtime with the tumor and the stromal compartments.

The emergence of technologies allowing single cell multiomics profiling has exponentially increased our understanding of the numerous cellular and molecular networks regulating carcinogenesis and tumor progression. However, most single cell-based high-throughput analytical tools require tissue disruption and single cell isolation, resulting in loss of information about the spatial organization of cells and cell-cell interactions<sup>7</sup>. Because the location and arrangement of specific immune cells in the TME have diagnostic and prognostic value, technologies allowing spatial resolution are an essential complement of single cell-based immune profiling techniques.

Traditionally, imaging techniques like immunohistochemistry (IHC) and multiplex immunofluorescence (mIF) have been restricted to a small number of biomarkers that can be visualized simultaneously. This limitation has hampered the study of the spatiotemporal dynamics of tumor-infiltrating immune cells, which are typically defined by several phenotypic markers. Recent advances in imaging and analytical tools have expanded the possibilities of multiplexing. New antibody-based labeling technologies like histo-cytometry and imaging mass cytometry have been used to spatially separate up to 12 and 32 biomarkers, respectively<sup>8,9</sup>. Mass spectrometry imaging, a technique not requiring labeling, has the potential to image thousands of biomarkers simultaneously in a single tissue section<sup>10,11</sup>. Although these techniques have already shown great potential for dissecting the tissue immune landscape in cancer, they use

highly sophisticated and expensive equipment and software and are not readily accessible to the majority of researchers.

Alternatively, the multiplexing capability of traditional IHC and mIF has been expanded through the use of serial imaging, sequential rounds of labeling, and spectral imaging<sup>7,12-16</sup>. These techniques generate multiple images from the same or from serial tissue sections that can be consolidated into virtual multiparameter slides using image analysis software. As a result, the number of markers that can be visualized and analyzed simultaneously increases.

Here, we propose a strategy for the rational design of tissue multiplex assays using commercially available reagents, affordable microscopy equipment, and user-friendly software (**Figure 1**). This methodology integrates serial imaging, sequential multiplex labeling, whole tissue imaging, and tissue alignment to generate virtual multiparameter slides that can be used for automated quantification and mapping of immune cells in tissue sections. Using this strategy, we created one virtual slide comprising 11 biomarkers plus two frequently used histological stains: hematoxylin and eosin (H&E) and picosirius red (PSR). Multiple immune cell populations were identified, located, and quantified in different tissue compartments and their spatial distribution resolved using tissue heatmaps. This strategy maximizes the information that can be gained from limited clinical specimens and is applicable to formalin-fixed paraffin-embedded (FFPE) archived tissue samples, including whole tissue, core needle biopsies, and tissue microarrays. We propose this methodology as a useful guide for designing custom assays for identification, quantification, and mapping of immune cell populations in the TME.

## **PROTOCOL:**

Three serial FFPE sections from resected hepatitis B virus (HBV)-associated human hepatocellular carcinoma were obtained from the Centre Hospitalier de l'Université de Montréal (CHUM) Hepatopancreatobiliary Cancer Clinical Database and Biological Specimen Repository (HBP Biobank). Patients participating in this tissue bank provided informed consent. This study was approved by the institutional ethics committee (Protocol number 09.237) and performed in accordance with the Declaration of Helsinki.

### **1. Hematoxylin and eosin (H&E) staining protocol**

NOTE: The H&E staining was performed by the molecular pathology core facility of the Centre de Recherches du Centre hospitalier de l'Université de Montréal (CRCHUM) using the Shandon multiprogram robotic slide stainer using the following program.

1.1. For deparaffinization, immerse slides 3x for 2.5 min each in xylene substitute.

CAUTION: Xylene substitutes are flammable, skin irritants, and harmful if inhaled.

1.2. For rehydration, immerse slides in 100% ethanol 3x for 2.5 min each. Wash for 1 min in double distilled water (ddH<sub>2</sub>O) to rehydrate.

133  
134 1.3. Incubate for 1 min in hematoxylin. Wash 3x for 1 min each in ddH<sub>2</sub>O.

135  
136 1.4. Incubate for 5 s with eosin. Wash 30 s with 95% ethanol. Wash 2x for 1 min with 100%  
137 ethanol.

138  
139 CAUTION: Ethanol is flammable and an eye irritant. Eosin is an eye irritant.

140  
141 1.5. For dehydration, immerse 3x for 1.5 min each in the xylene substitute. Mount slides  
142 manually.

143  
144 Note: The estimated time for executing this part of the protocol is 30 min.

## 145 146 **2. Multiplex immunofluorescence staining protocol for FFPE sections**

147  
148 NOTE: This protocol was adapted from Robertson et al.<sup>17</sup>.

### 149 150 2.1. Deparaffinization and rehydration

151  
152 NOTE: Before antibody-mediated labeling of FFPE sections by IHC or mIF, the paraffin should be  
153 removed. Failure to efficiently remove the paraffin results in suboptimal staining.

154  
155 2.1.1. Place 4 µm of FFPE tissue section slides into glass slide holders. Under the fume hood,  
156 immerse the slides in a Coplin jar containing 37 °C prewarmed xylene for 10 min.

157  
158 CAUTION: Xylene is flammable, a skin irritant, and harmful if inhaled.

159  
160 2.1.2. Manually agitate the slides for 10 s every 2 min. Repeat 1x in fresh xylene for another 5  
161 min.

162  
163 2.1.3. In the chemical hood, immerse the slides sequentially for 5 min in each of the following  
164 solutions: 1) xylene:ethanol (1:1 v/v); 2) 100% ethanol; 3) 70% ethanol; 4) 50% ethanol; 5) 30%  
165 ethanol; 6) phosphate-buffered saline (PBS).

166  
167 NOTE: Keep the slides in PBS until ready to perform the antigen retrieval. Keep the dewaxed  
168 sections hydrated at all times. Drying out will cause nonspecific antibody binding and therefore  
169 high background staining.

### 170 171 **2.2. Heat-induced antigen retrieval**

172  
173 NOTE: Antigens can be masked upon formalin-fixation, preventing antibody binding and  
174 consequently visualization. The use of antigen unmasking buffers and procedures partially  
175 reestablish the native conformation of epitopes and thereby restores antibody recognition. The  
176 type of antigen retrieval buffer and duration should be optimized for the specific assay conditions

(e.g., target, antibody, tissue, etc.).

2.2.1. Immerse dewaxed slides in a Coplin jar containing the antigen retrieval solution (recipe in **Table of Materials**).

2.2.2. Place closed Coplin jar into an electric pressure cooker with tap water. The water level should not exceed half the height of the jar so that the water does not mix with the antigen retrieval solution.

2.2.3. Close the lid and the pressure valve of the cooker. Select high pressure for 10 min and start. When done, unplug the cooker, release the pressure, open the lid, and keep the jar inside the cooker for 30 min, allowing the slides to cool.

### 2.3. Blocking of nonspecific binding

2.3.1. Transfer the rack with the slides to a Coplin jar filled with PBS. Rinse off the antigen retrieval buffer with PBS 2x for 5 min each.

2.3.2. Encircle the tissue sections with a PAP pen to create a hydrophobic barrier. Immerse the slides in a Coplin jar containing 0.1 M glycine in PBS. Incubate for 15 min at room temperature (RT).

NOTE: Glycine saturates the aldehyde groups generated during antigen retrieval. These groups could bind primary and secondary antibodies unspecifically.

2.3.3. Rinse off the glycine solution by washing 2x with PBS for 5 min. Place the slides into a humidity chamber and add enough blocking solution to cover all the tissue sections. Avoid overflowing the hydrophobic barrier. Incubate for 30 min at RT.

NOTE: The recipe for the blocking solution can be found in the **Table of Materials**. The blocking solution should contain a protein (e.g., BSA) to block nonspecific binding sites. It can also incorporate detergents like Triton X-100 or Tween 20 that reduce hydrophobic interactions between antibodies and tissue targets, thereby making antigen recognition more selective. The addition of 10% total serum from the species where the tissue comes from would block Fc receptors, and thus reduce nonspecific antibody binding. Finally, addition of 10% of serum from the species the secondary antibodies were raised in would minimize direct nonspecific attachment of secondary antibodies to the tissue section.

### 2.4. Immunofluorescence labeling

2.4.1. Rinse with PBS-Tween (0.1% v/v) 2x for 5 min each and place the slides back in the humidity chamber.

2.4.2. Add the cocktail of primary antibodies resuspended in blocking solution. Incubate

overnight at 4 °C. Primary and secondary antibodies used for this study are listed in **Table of Materials**.

NOTE: The cocktail of primary antibodies should contain either antibodies raised in different species, or from the same species but of different isotypes. For a list of the primary-secondary antibody pairs used in this study consult **Table 2**. Details of all antibodies used are in the **Table of Materials** and **Table 2**.

2.4.3. Rinse with PBS-Tween (0.1% v/v) 3x for 5 min and place the slides back into the humidity chamber. In the dark, add the cocktail of secondary antibodies and incubate for 1 h at RT.

NOTE: When the primary antibodies are from different species, the secondary antibodies should be selected so that each of them only binds to one of the primary antibodies and not to one another. This is commonly achieved by using secondary antibodies all raised in the same species as long as this species differs from the species where the primary antibodies were generated. In cases where the primary antibodies were raised in the same species but have different isotypes, isotype-specific secondary antibodies should be used.

2.4.4. Rinse with PBS-Tween (0.1% v/v) 3x for 5 min each. Rinse with 1x in ddH<sub>2</sub>O. Remove excess liquid and mount in mounting media with DAPI. The volume used depends on the size of the section. Usually 40 µL is enough to cover the surface of a regular microscopy slide.

2.4.5. Place the cover slide onto the section and gently squeeze out the excess mounting media avoiding bubble formation. Let the slides dry for 20 min at RT in the dark and store at 4 °C until ready for acquisition.

2.4.6. Acquire images for all the channels using the whole slide scanner (see **Table of Materials**).

NOTE: The antibodies were validated using human hepatocellular carcinoma tissue as a positive control. For each primary antibody, three serial sections were stained with either primary antibody, isotype control, or only blocking solution respectively with no variation in the rest of the staining protocol. The acquired images were compared to establish the specificity of the staining. The staining was considered specific when the signal in the section incubated with primary antibody had the expected pattern and was easily distinguishable from the background. Primary antibodies giving a high background signal or labelling tissue components in the isotype and no primary antibody sections were considered nonspecific. The estimated time for completing this part of the protocol is 2 days. Required controls include: (1) Isotype Control to establish the contribution of nonspecific binding of the primary antibody to the background signal. One section is stained in the same way as the other sample tissues except that it is incubated with an antibody with the same isotype and origin of the primary antibody but specific for a target that is absent in the tissue section. If the appropriate isotype control antibody is not available, it can be replaced by total IgG from the same animal where the primary antibody was raised in; (2) No Primary Antibody Control (i.e., negative control) to establish the specificity of the staining and to estimate the contribution of nonspecific binding of secondary antibodies to

the background signal. In this case, the control section is stained in the same way as the other sections except that no primary antibody is added; (3) Positive Control to establish that the staining works. In this case, the staining is performed on a tissue section that is known to express the marker recognized by the primary antibody.

### 3. Picro-sirius red (PSR)/fast green staining protocol

NOTE: The goal of this staining is to visualize fibrillar collagens I and III in the FFPE tissue sections. This protocol was adapted from Segnani et al.<sup>18</sup>. All steps are performed in a chemical hood.

3.1. Perform the deparaffinization and rehydration of tissue sections similar to the multiplex immunofluorescence staining protocol for the FFPE sections (section 2.1).

NOTE: If the section to be stained has previously been used for immunofluorescence labeling and the paraffin has already been removed, the deparaffinization-rehydration steps are useful to remove the mounting media. DAPI is not removed using this procedure but it does not perceptibly interfere with the PSR staining.

3.2. Immerse the slides in a jar containing the picro-sirius red/fast green solution (recipe in **Table of Materials**) and incubate for 30 min at RT (more than 30 min results in nonspecific staining of the nuclei of hepatocytes).

3.3. Wash slides quickly in ddH<sub>2</sub>O (5 dips). Then, wash quickly in ethanol 100% (5 dips). Wash for 30 s in xylene-100% ethanol (1:1 v/v). Wash for 30 s in xylene. Mount with mounting media (see **Table of Materials**) before xylene has totally evaporated (this helps with the mounting).

NOTE: The estimated time for executing this part of the protocol is 1 h.

### 4. Elution of antibodies from tissue sections

NOTE: In order to reuse tissue sections in sequential labelling assays, the complete removal of primary and secondary antibodies is required. Bound antibodies were stripped as previously described<sup>13</sup>.

Preheat a water bath to 56 °C. Put the sections inside a jar containing stripping buffer (recipe in **Table of Materials**), close the lid, and seal it with paraffin film tape to prevent leaking during shaking.

4.1. Put the jar inside the water bath and incubate for 30 min with agitation.

4.2. Wash 4x for 15 min each in ddH<sub>2</sub>O at RT. Rinse with PBS-Tween (0.1% v/v).

4.3. Keep the sections hydrated in PBS-Tween or water until ready to reprobe the section with the second round of primary antibodies.



NOTE: The estimated time for executing this part of the protocol is 2 h.

4.4. Verify the efficiency of the antibody elution procedure.

NOTE: Before using the protocol for antibody elution in a sequential labelling assay, the efficiency of the removal of primary and secondary antibodies should be verified.

4.4.1. Perform the staining and image acquisition of a section with a given primary-secondary antibody pair of interest as indicated in the multiplex immunofluorescence staining protocol for FFPE sections (sections 2.1–2.4.6).

4.4.2. Upon image acquisition, perform elution of tissue-bound primary-secondary antibody complexes as indicated in sections 4.1–4.3.

4.4.3. Incubate the section with the same secondary antibody and same conditions used in step 2.4.3.

4.4.4. Perform washing, mounting, and image acquisition steps as indicated in 2.4.4–2.4.6.

4.4.5. Compare side by side images acquired before and after the stripping in order to establish whether or not the specific signal has disappeared.

NOTE: Comparison of images before and after antibody removal will validate the efficiency of the elution procedure. However, it is normal to see an increase in the background signal in all the channels, as well as diffusion of DAPI. This limits the number of rounds of stripping that can be executed on the same tissue section. Three rounds of stripping seem to be the maximum.

## 5. Image acquisition

5.1. Generate images using a whole slide scanner.

5.2. Use a 20x 0.75NA objective lens and a resolution of 0.3225  $\mu\text{m}/\text{pixel}$ .

## 6. Image analysis

NOTE: The method outlined here refers to the current example. Please refer to **Table 1** and the text to adapt to other specific samples.

6.1. Perform tissue alignment using the Tissualign module of the image analysis software (VIS in this protocol, see **Table of Materials**).

6.1.1. Open the image analysis software and click on the **Tissuealign** tab.

6.1.2. Import the images to be aligned into the **Slide Tray** by going to **File | Database** and select the first image to be aligned. Go back to the **Tissuealign** tab and load the image by clicking the **Load** button in the **Slide Tray**. The image will appear in the **Slide Tray** and in the workspace.

NOTE: Only the stack of interest should be loaded into the slide tray.

6.1.3. Repeat step 6.1.2 for all the images in the order to be aligned, loading them one by one. Once all the images of interest are loaded onto the slide tray proceed to link the images by pressing **Next** in the **Workflow Steps** in the ribbon.

6.1.4. Next, drag and drop the second image on top of the first image. The first and second images are now linked. Repeat this step for the other images to be aligned, one by one, in an orderly fashion. The name of the first image will change, indicating that it has been linked to the other images. Simultaneously, the linked images will be displayed in the workspace on the right of the slide tray.

6.1.5. At this point, align the images either using automatic alignment, semiautomatic alignment, or manual alignment. It is always preferable to try automatic alignment first. For automatic alignment press the **Next** button in the workflow steps (step 3) in the ribbon.

6.1.6. Review the automatic alignment by navigating different locations of the tissue and visually verifying that the corresponding structures in different images are arranged in the same way in the two dimensions of the image.

6.1.7. If the result of the automatic alignment is not satisfactory, improve it using pins (use a minimum of three pins per image) indicating homologous tissue features in the linked images. Once the pins are placed at homologous locations in the linked images, the user has two choices: semiautomatic alignment or manual alignment. For semiautomatic alignment click on the button **Auto-align** based on the current pinpoints in the ribbon. For manual alignment, click the button **Apply Pins** on the ribbon.

6.1.8. When satisfied with the alignment click on the **Next** button in the workflow steps and save the composite image in the database.

NOTE: Aligning six slides spanning 11 markers plus the H&E and PSR images took 15 min in the analysis presented.

6.2. Perform tissue detection using the user-defined protocol Analysis Protocol Package 1 (APP 1, Table 1).

6.2.1. Open the **Image Analysis** module of the software by clicking the **Image Analysis** tab in the ribbon.

6.2.2. Import the composite (aligned) image by going to **File | Database** and selecting the image

of interest and clicking back the **Image Analysis** tab.

6.2.3. Open the APP selection dialog by clicking on the **Open APP** icon and select which Analysis Protocol Package (APP) to use. In this case select **APP 1** for tissue detection.

6.2.4. Once APP 1 is opened, confirm that APP1 is working properly by going to a selected tissue location and clicking on the **Preview** button. If the results are satisfactory, go to the next step.

6.2.5. Click to run APP 1 and process the image using the selected APP.

6.2.6. Export the data (e.g., images, measurements, etc.) when the analysis is done by clicking **File/Export**.

NOTE: APP 1 creates a region of interest (ROI) delineating the tissue (ROI Tissue) and calculates the area of the tissue.

6.2.7. Save the modified image with the newly created ROI by going to **File | Save**.

NOTE: Detecting the tissue and creating a ROI with APP 1 in the provided example took 5 min in the image analysis station described. The area of the tissue processed was 3.2 cm<sup>2</sup>.

6.3 Perform tissue segmentation into Stroma and Parenchyma using APP 2 (**Table 1**).

NOTE: APP 2 works on the predefined ROI Tissue. APP 2 segments the tissue into the ROIs Stroma and Parenchyma.

6.3.1. Open the Image Analysis module by clicking the **Image Analysis** tab in the ribbon.

6.3.2. Import the image containing the ROI tissue by going to **File | Database** and selecting the image saved in step 6.2.7. Go back to the **Image Analysis** tab and load the image by clicking the **Load** button in the **Slide Tray**. The image will appear in the **Slide Tray** and in the workspace.

6.3.3. Open APP 2 using the APP selection dialog as in 6.2.3.

6.3.4. Preview APP 2 by processing in a selected field of view. If the results are satisfactory, run APP 2 on the full image by clicking the **Run** button. As the output of APP 2, the ROI tissue is segmented in the ROIs Stroma and Parenchyma and their respective areas determined. Export results as in 6.2.6. Save the modified image as in 6.2.7.

NOTE: Segmenting the tissue in Stroma and Parenchyma using APP 2 took 4 h in the analysis station presented. The area of the tissue processed was 3.2 cm<sup>2</sup>.

6.4. Identify and quantify FoxP3<sup>hi</sup>CD4<sup>+</sup> cells using the user-defined protocol APP 3 (**Table 1**).

NOTE: APP 3 works on the predefined ROIs Stroma and Parenchyma.

6.4.1. Open the Image Analysis module and import the image containing the ROIs Stroma and Parenchyma as in 6.3.1 and 6.3.2. Open APP 3 using the APP selection dialog as in 6.2.3.

6.4.2. Preview APP 3 processing in a selected field of view enriched in FoxP3<sup>hi</sup>CD4<sup>+</sup> cells. If the results are satisfactory, run APP 3 on the full image. As the output of APP 3, all the individual FoxP3<sup>hi</sup>CD4<sup>+</sup> objects will be labeled and their tissue coordinates stored. Densities of FoxP3<sup>hi</sup>CD4<sup>+</sup> objects in the ROIs Stroma and Parenchyma will be determined. Export the results as in 6.2.6.

6.4.3 Perform tissue heatmapping of FoxP3<sup>hi</sup>CD4<sup>+</sup> labelled objects.

6.4.3.1. Open the user-defined protocol FoxP3<sup>hi</sup>CD4<sup>+</sup> MAP using the APP selection dialog as in 6.2.3.

NOTE: FoxP3<sup>hi</sup>CD4<sup>+</sup> MAP uses the coordinates of FoxP3<sup>hi</sup>CD4<sup>+</sup> labelled objects for generating density heatmaps. Identifying and counting FoxP3<sup>hi</sup>CD4<sup>+</sup> labeled objects using APP 3 took 25 min in the image analysis station described. The area of the tissue processed was 3.2 cm<sup>2</sup>.

6.4.3.2. Run FoxP3<sup>hi</sup>CD4<sup>+</sup> MAP by pressing the **Run** button. Export the tissue heatmap by clicking **File | Export | Working Area**.

NOTE: Mapping FoxP3<sup>hi</sup>CD4<sup>+</sup> labeled objects using FoxP3<sup>hi</sup>CD4<sup>+</sup> MAP took 5 min in the image analysis station described.

6.5. Identify and quantify CD8<sup>+</sup>, CD68<sup>+</sup>, MPO<sup>+</sup>,  $\alpha$ SMA, and CD34<sup>+</sup> objects using the user-defined protocols APP 4, APP5, APP6, APP7, and APP 8, respectively (**Table 1**) as done in section 6.4 to 6.4.3.2 loading the APP of interest in each case.

NOTE: APPs 4 to 8 work on the predefined ROIs Stroma and Parenchyma.

## REPRESENTATIVE RESULTS:

### Overview of the strategy for visualizing, quantifying, and mapping cell populations of interest in the TME

To quantify cell populations of interest (COIs) in different tissue compartments (TCs) and to characterize their spatial organization, we designed a workflow that integrates affordable and easy to use techniques and maximizes the positional information that can be obtained from precious FFPE clinical specimens (**Figure 1**). First, serial whole tissue FFPE sections were stained for visualization of COIs (e.g., immune cells) and TCs (e.g., stroma versus parenchyma) (**Figure 1**, step 1). The number of consecutive sections to be stained should be kept to the minimum that allows visualization of the cells of interest or tissue features needed for addressing the research question. The smaller the number of serial sections, the higher the tissue architecture resemblance and concordance across contiguous sections. In addition, the multiplexing capability can be expanded through reuse of fluorescently stained sections through stripping and reprobing

techniques<sup>19</sup>.

Once the staining steps were done, a whole slide scanner was used to digitize the images. Images acquired from serial sections were aligned and consolidated into a virtual multiplex slide in an automated fashion (**Figure 1**, section 2). Next, a ROI for the ROI tissue was delineated with a user-defined protocol that identified tissue-associated pixels (TAPs) (**Figure 1**, step 3). Subsequently, the ROI tissue was segmented into TCs defined as additional ROIs. (**Figure 1**, step 4). Next, user-defined protocols detected and quantified COIs in different TCs (**Figure 1**, step 5). Finally, tissue heatmaps of COIs were generated based on their densities and their tissue coordinates (**Figure 1**, step 6).

[Insert Figure 1 here]

### **Imaging COIs and TCs**

Three serial FFPE whole tissue sections of resected tumor from a subject with HBV-associated hepatocellular carcinoma were stained in one or more rounds of staining as in **Figure 2A**. Section I was stained with H&E to show the tissue architecture, cell morphology, and to determine clinically relevant parameters such as type of malignancy, tumor grade, and overall assessment of immune infiltration (**Figure 2C**). In contiguous section II, two rounds of mIF were used for labeling liver parenchymal and non-parenchymal cells (**Figure 2A**). In the first round, normal and tumor vessels were visualized using CD34 staining of endothelial cells. Additionally, epithelial cells (hepatocytes and cholangiocytes) were identified using cytokeratin 8/18, and fibrogenic activated hepatic stellate cells were identified as  $\alpha$ SMA+ cells (**Figure 2C**). Following image acquisition, tissue sections were stripped and reprobed with antibodies against macrophages (CD68), and myofibroblasts (desmin). To better characterize the tumor immune infiltrate, adjacent serial section III was stained using two rounds of mIF for the cellular markers CD3, CD4, CD8, forkhead box P3 (FoxP3), and myeloperoxidase (MPO). In all cases DAPI was used as a nuclear counterstain. Finally, section III was stained with PSR stain and counterstained with fast green to visualize fibrillar collagen and segment the tissue into stroma and parenchyma (**Figure 2C**).

A whole slide scanner equipped with a 20X objective lens was used to digitize stained sections and to create virtual slides. Six images were acquired from the three serial sections (**Figure 2B**) and the virtual slides subsequently analyzed using the VIS software according to the schematic representation in **Figure 1**.

### **Image Analysis**

The image analysis comprised five steps: 1) tissue alignment; 2) tissue detection; 3) tissue segmentation; 4) automated quantification of COIs; and 5) tissue heat mapping. All protocols for image analysis were developed using the Author module of the image analysis software and are referred to in the text as APP. All APPs in this study were designed using the Author module.

### **Tissue alignment**

Six virtual slides from three serial sections, spanning 11 markers plus H&E and PSR stains, were

loaded into the Tissualign module of the image analysis software. Next, the images were linked, aligned, and coregistered in an automated fashion, generating an 11-plex plus H&E and PSR virtual composite image, containing all the layers of the individual images (**Figures 2A–C**). Alignment was accurate in the case of images originating from adjacent serial sections, showing corresponding tissue structures positioned and arranged in a homologous fashion upon alignment (**Figure 2C** and **Figure S1A**). Furthermore, the alignment was precise at the individual cell level for images originating from the same section (**Figure S1B**). The automatic alignment of the six slides took 15 min to execute in our VIS station. The time is dependent on the number of slides, the size and complexity of the individual images, and the overall similarities among the images to be aligned. The time for automatic alignment depends on the number, size, complexity, and similarity of the images to be aligned. The alignment of the above-mentioned six virtual slides took 15 min in our VIS station.

[Insert Figure 2 here]

### **Tissue Detection**

Once the images were linked and aligned, we sought to identify the TAPs (**Figure 3A**). To design an APP for the automated detection of TAPs (APP 1, **Table 1**), we took advantage of two properties that differentiate TAPs from pixels not associated with tissue. First, the DAPI signal (blue band) is restricted to the nuclei, which are located exclusively in the tissue, meaning that all DAPI+ pixels are a subset of TAPs. Second, TAPs have higher autofluorescence signal in the green and yellow bands compared to pixels not associated with the tissue. Consequently, we developed APP 1 for tissue detection (**Table 1**), which detects the TAPs based on baseline signal in these channels using simple thresholding techniques. Thresholds for the blue, green, and yellow bands were set so that TAPs had background intensity values above the thresholds, while pixels not associated with the tissue had values below. APP 1 for tissue detection was applied to image IIA, which contains layers in the blue, green, and yellow channels (**Figure 3A**). As outputs of APP 1, a bright green mask was laid down on top of the TAPs, and a ROI called “Tissue” was delineated (output, **Figure 3A**). Furthermore, the area of the tissue was determined as a quantitative output variable. Because APP 1 does not incorporate the pixels not associated with the tissue into the ROI Tissue, they were excluded from subsequent analysis based on this ROI (**Figure 3A**). The precision of APP 1 at identifying TAPs is shown in **Figure 3A**.

### **Tissue segmentation and delineation of ROIs for TCs**

Next, we proceeded to define different compartments inside the ROI tissue by segmenting the tissue into stroma versus parenchyma. We used the PSR stained image (IIC, **Figure 2C**), where the stroma can be defined as the area associated with the deposition of fibrillar collagens (red band), the parenchyma as the area where fibrillar collagens are absent, and the fast green counterstaining dye prevails (green band) (**Figure 3B**). We created APP 2 (**Table 1**) to digitally delimit the TCs Stroma and Parenchyma. This APP works on the predefined ROI Tissue (output, **Figure 3A**) and uses representative stroma and parenchyma areas for training the Classifier tool integrated in the Image Analysis module. The trained Classifier assigns the pixels to either a stroma or a parenchyma label (salmon and green, respectively, **Figure 3B**). Upon classification of pixels, APP 2 executed morphological operations aiming at defining the ROIs Stroma and

Parenchyma (**Figure 3B** and **Table 1**). The performance of APP 2 at classifying pixels and generating the respective ROIs is shown in **Figure 3B**. Additionally, APP 2 quantifies the area of the stroma and the parenchyma. Finally, even though the segmentation is done using the PSR stained section, the outlined stroma and parenchyma regions can be transferred to any image aligned to the PSR image.

[Insert Figure 3 here]

### **Automated quantification of COIs**

Next, we proceeded to identify, locate, and quantify COIs in the ROIs Stroma and Parenchyma. APPs 3 to 8 (**Table 1**) were created to locate and count the following COIs: CD4+FoxP3+, CD8+, CD68+, MPO+,  $\alpha$ SMA+, and CD34+ cells, respectively. APP 3 was designed to locate and count CD4+FoxP3+ cells (image IIIA, **Figure 2C**) as surrogate markers of regulatory T cells (Tregs). This protocol detects colocalization of the signal from the nuclear transcription factor FoxP3 (red band) and the DNA labeling dye DAPI (blue band). Given that recently activated T cells upregulate FoxP3, to enrich for Tregs we set thresholds for preselecting only bright FoxP3+ cells (FoxP3<sup>hi</sup>). Next, out of all preselected DAPI+FoxP3<sup>hi</sup> cells, only those that were surrounded by bright ring-shaped CD4 signals (green band) were labelled and counted as FoxP3<sup>hi</sup>CD4+ cells (pink label, **Figure 4A**). The density of FoxP3<sup>hi</sup>CD4+ cells in the ROIs Stroma and Parenchyma were determined as quantitative output variables of APP 3 (**Figure 4A**).

Similarly, APPs 4 to 6 were designed for the detection of CD8+, CD68+, and MPO+ cells. These APPs share the same baseline design for detecting and quantifying COIs. Specifically, COIs are identified based on signal intensity from the specific cell population biomarker, and then several postprocessing morphological steps are executed to delineate individual cells (**Table 1**). The individual cells or COIs are labelled, counted, and their tissue coordinates registered. APPs 4 to 6 also determine the density of the COIs in the ROIs Stroma and Parenchyma (**Figure 4B–D**).

The quality of our DAPI staining was not good enough for integrating nuclei segmentation into APPs 2 to 6, so we cannot ensure that all individually labelled objects are individual cells. For this reason, we expressed the density of cells in counts of labeled objects/mm<sup>2</sup> (**Figure 4**). However, cell aggregates were successfully separated into individual cells in the postprocessing steps built into APPs 3 to 6, and extensive visual inspection showed that most labeled objects corresponded to single cells.

For detecting  $\alpha$ SMA+ and CD34+ area, we developed APPs 7 and 8, respectively (**Table 1**). Both APPs detect the specific signal based on thresholds and determine the percentage of positive area in the ROIs Stroma and Parenchyma (**Figure 4E–F**).

One of the most interesting possibilities of generating virtual multiplex slides is the analysis of colocalization expression. We generated APP 10 to detect colocalization between  $\alpha$ SMA and desmin, two markers co-expressed by myofibroblasts in the liver. APP 10 uses thresholds for finding pixels positive for  $\alpha$ SMA, desmin, and  $\alpha$ SMA plus desmin (**Table 1**). As quantitative output variables, APP 10 determines the  $\alpha$ SMA+ area, the desmin+ area, and the area of colocalized

expression of these two markers (**Figure S3**).

[Insert Figure 4 here]

As an alternative to quantifying the COIs in the TCs Stroma and Parenchyma, we determined the density of immune cells in the different malignant nodules named 1 to 4 (**Figure 5A, H, and I**). The ROI for each nodule was manually delineated as indicated in **Figure 5A**. Distinctive tissue immune signatures characterized each nodule, further revealing the intrinsic heterogeneity of the TME.

### **Tissue Heatmaps**

As mentioned above, APPs 3 to 8 store the tissue coordinates of every individually labelled object. This feature allows the automated generation of tissue maps where regions of high density of a given cell population are displayed as hot spots (red), and regions with relatively low density as cold spots (dark blue). Intermediate density values are assigned colors according to the color scale shown in **Figure 5**. Tissue heatmaps were generated by APPs that divided the images into circles of 50  $\mu\text{m}$  diameter and assigned a color according to the relative density of a given COI inside the circle. As displayed in **Figure 5B–G**, the positioning patterns and intensity distribution of the different COIs in the TME was quite varied. Furthermore, at the level of individual nodules, the arrangement of different populations in the tissue area was unique (**Figure S2A–C**). To provide an example of the power of this technique and to visualize the spatial organization of hot spots from different populations in the same nodule, the hot spots from individual cell types were manually extracted and mapped together onto the outline of nodule 2 (**Figure S2, Figure D, and Figure E**).

[Insert Figure 5 here]

### **FIGURE AND TABLE LEGENDS:**

**Figure 1: Schematic representation of the strategy for visualizing, quantifying, and mapping immune cells in the TME.** (1) Serial whole tissue sections were stained for labeling COIs and TCs. Stained whole tissue sections were digitized using a whole slide scanner. (2) Images acquired from serial sections were linked, aligned, and coregistered in an automated fashion using a Tissuealign analysis module. A composite image was generated from the high-precision alignment of individual images. (3) A user-defined protocol was used for automated detection of tissue-associated pixels (TAPs) in the composite image. (4) The tissue was segmented into TCs (e.g., stroma and parenchyma) defined as ROIs. (5) User defined protocols were used for the automated detection and quantification of COIs in different TCs. (6) Tissue heatmaps of COIs were generated.

**Figure 2: Staining of serial tissue sections and image alignment.** (A) Summary of stainings done on three serial sections for visualization of COIs and TCs. Numbers in brackets indicate image designation. For sections II and III, tissues were stripped and reprobbed with a second cocktail of antibodies. (B) Overview of six individual whole tissue images before and after tissue alignment (left and right, respectively). Scale bar = 3,500  $\mu\text{m}$ . (C) Zoomed view of aligned images. Scale bar



= 80  $\mu$ m.

**Figure 3: Automated tissue detection/segmentation and generation of respective ROIs.** (A) Image IIA was used to identify the TAPs (left image, scale bar = 6,000  $\mu$ m). A bright green mask was assigned to the TAPs using APP 1 (**Table 1**) generating a ROI called Tissue (output 1). Right, inset shows zoomed view demonstrating the precision of APP 1 at detecting TAPs. Scale bar = 350  $\mu$ m. (B) The ROI Tissue (output 1) is segmented into stroma and parenchyma using APP 2. The image on the left shows a view of the ROI Tissue segmented into ROI stroma (salmon) and ROI parenchyma (green). Scale bar = 4,500  $\mu$ m. On the right, zoomed views of inset for ROI Tissue, the original PSR staining (image IIIC), and the ROIs stroma and parenchyma. Scale bar = 250  $\mu$ m.

**Figure 4: Identification and quantification of COIs in the TCs stroma and parenchyma.** (A–F) Automated detection and quantification of CD4+FoxP3+, CD8+, CD68+, MPO+,  $\alpha$ SMA+, and CD34+ COIs in the ROIs Stroma and Parenchyma using protocols 3, 4, 5, 6, 7, and 8, respectively (**Table 1**). Shown on the left are the original images, in the middle the processed images, and on the right the quantifications. For **Figures 4A–D**, scale bar = 40  $\mu$ m. For **Figures 4E and F**, scale bar = 350  $\mu$ m.

**Figure 5: Tissue heatmaps of COIs in the TME.** (A) Picrosirius Red staining showing location of nodules 1, 2, 3, and 4. (B–G) Tissue heatmaps for CD4+FoxP3+, CD8+, CD68+, MPO+, CD34+, and  $\alpha$ SMA+ COIs, respectively. Dark blue indicates relative low density, and red indicates relative high density. Intermediate density values are assigned colors according to the shown color scale. (H and I) Quantification of COIs in nodules 1, 2, and 3 + 4 organized per cell type and per nodule, respectively.

**Supplementary Figure S1: Validation of tissue alignment.** (A) CD34 staining (in red) done on section II (input 1) is used for generating a CD34 mask in green (output 1). The green mask (output 1) is overlaid on the H&E image from the aligned serial section I (input 2). The merge image shows perfect correspondence of vascular structures. Scale bar = 50  $\mu$ m. (B) Image IIIA showing the merge of DAPI, CD4, and FoxP3 (input 1) was used to generate a label for CD4+FoxP3+ cells (output 1 in magenta). Output 1 label was transferred onto aligned image IIIB (input 2) and shows perfect correspondence between the pairs FoxP3/DAPI, and CD4/CD3 in the merge image. Scale bar = 15  $\mu$ m.

**Supplementary Figure S2: Zoomed view of tissue heatmaps.** (A–C) Tissue heatmaps for CD4+FoxP3+, CD8+, CD68+, and MPO+ cells in nodules 1–4. Scale bars in nodules 1, 2, and 3 + 4 represent 1,500  $\mu$ m, 700  $\mu$ m, and 500  $\mu$ m respectively. (D) Outline of nodule 2 with black solid line. (E) Hot spots for CD4+FoxP3+, CD8+, CD68+, and MPO+ cells in nodule 2 were extracted and mapped together onto the nodule 2 outline defined in D.

**Supplementary Figure S3: Colocalization Analysis.** (A) On the left and middle are images of  $\alpha$ SMA label in green and desmin label in red respectively. On the right is a  $\alpha$ SMA/desmin double positive area in yellow. (B) Quantification of  $\alpha$ SMA+ area, desmin + area, and  $\alpha$ SMA/desmin double positive area. Scale bar = 150  $\mu$ m.

**Table 1: General parameters used for the design of APPs employed for image analysis.** The parameters specified in this table are adjusted to the unique characteristics of the images used in this analysis (e.g., background, artifacts, etc.) and may not be applicable to other images. Because the post-processing steps mentioned were defined for the specific images analyzed in this study, they are intentionally not detailed. The user should customize the APPs to the images to be analyzed.

**Table 2: Primary-Secondary Antibody Pairs for mIF.**

## **DISCUSSION:**

Simple, accessible, and easy to execute multiplexing techniques that allow spatial resolution of immune cells in tissue sections are needed to map the immune landscape in cancer and other immunological disorders. Here, we describe a strategy that integrates widely available labeling and digital analysis techniques to expand the multiplexing capability and multidimensional assessment of imaging assays<sup>12,13,17,19</sup>. The staining of three serial sections for different markers, and the reuse of sections through stripping and reprobing techniques, enabled us to visualize 11 parameters in addition to H&E and PSR stains. Six images from these sections were aligned in an automated fashion using the tissue alignment module. The alignment was precise at the individual cell level for images originating from the same section and highly concordant for images originating from neighboring sections. Virtual multiplexing enabled us to determine how markers visualized in one section relate spatially to markers visualized in another contiguous section. While some of the stainings labelled COIs, others labelled TCs, allowing us to quantify COIs in the different TCs. The use of software tools for the automated quantification of COIs greatly simplified and accelerated the processing of images. Moreover, digital analysis was applied to whole tissue sections instead of selected fields of view, resulting in an unbiased representation of the TME. Furthermore, because the tissue coordinates of COIs were registered, it was possible to generate tissue heatmaps.

There are several areas in this protocol where troubleshooting may be needed. First, poor antigen retrieval can affect the quality of mIF, therefore the type of antigen retrieval buffer and duration should be optimized for the specific assay/biomarker conditions used. Second, the type of blocking solution used should be adapted to the tissues/antigen/species of primary and secondary antibodies. In our hands, the addition of 10% total serum from the species where the tissue comes from blocked Fc receptors, and thus reduced nonspecific antibody binding. Addition of 10% of serum from the species the secondary antibodies were raised in would minimize direct nonspecific attachment of secondary antibodies to the tissue section. Third, validation of the specificity of the primary and secondary antibodies using the proper positive and negative controls is essential. Fourth, increased autofluorescence in some channels and diffusion of DAPI upon primary antibody stripping are also common. To address the enhanced autofluorescence, we used primary/secondary antibody pairs where the specific signal had intensity values at least 5x that of the background. Finally, some high affinity antibodies cannot be eluted with regular stripping procedures. In this case, we recommend using such antibodies in the last round of labeling. The user may have to try different staining sequences to find the optimal configuration

for the antibodies of interest. Efficiency of stripping should be confirmed before proceeding to a second or third round of labeling.

The main limitation and challenge of this strategy is finding the right combinations of primary and secondary fluorescent antibodies for the markers of interest. Finding primary antibodies raised in different species or with different isotypes that could be used simultaneously is limited by what is commercially available. Most whole slide scanners are equipped with lamps and filters that allow imaging a maximum of five channels, and secondary antibodies in the right species and right fluorophore are not always available. We partially overcame these limitations using serial stainings and sequential labeling. Several antibody combinations may need to be tested to arrive at the best combination for the markers of interest. Another limitation is the quality of the DAPI staining, because stripping and probing may not always allow performing nuclei segmentation.

The tissue align module requires minimal training and no programming skills from users. The software theoretically allows alignment of an unlimited number of images. However, precise alignment depends on relatedness of sections, where closer sections that are more histologically concordant are more accurately aligned. We used the Author module of VIS for generating the APPs. Basic knowledge of image analysis is needed for creating APPs, but this is equally the case when using any other image analysis software. The unique advantages of VIS as compared to other image analysis software include automated alignment of images from sections prepared using different methods (e.g., IF, histochemistry, IHC). This allows colocalization studies of multiple markers of interest using virtual multiplexing. Furthermore, the flexible and user-friendly design of APPs allows user-specific customization. Automated quantification and mapping, and the possibility of processing whole tissue sections, saves time and reduces bias compared to manual counting by visual inspection.

This strategy remains a very useful research tool for tissue immunology in the context of cancer and autoimmunity but remains unvalidated for clinical use. With additional standardization and validation, it can be used in the future for multiple applications (e.g., to map the immune landscape in cancer to predict and monitor the response to immunotherapeutic agents). It can also be adapted to different inflammatory conditions (e.g., inflammatory bowel disease) to combine pathological evaluation with prognostic biomarkers.

The main critical steps in this protocol are the efficiency/specificity of the labeling and the robustness of the designed APPs for the intended use or biomarker. Hence, regular validation by visual inspection, especially upon designing a new APP, is essential. The efficient use of multiple rounds of stripping and reprobing or different types of stains on the same section are critical components and can be tissue or section specific. Verifying the efficiency of such processes before proceeding with large batch analysis is critical.

In summary, we provide a strategy that maximizes the quantitative and spatial information that can be obtained from valuable clinical tissue samples. The resources, equipment, and knowledge required to implement this methodology are widely accessible. We propose this methodology as

a useful guide for planning assays aiming at identifying, quantifying, and mapping immune cell populations in the TME.

#### **ACKNOWLEDGMENTS:**

We thank the study participants. We thank Louise Rousseau, coordinator of the HBP biobank for recovery of the tissue samples and all associated clinical information. We acknowledge the molecular pathology and cell imaging core facility at the CRCHUM for excellent technical assistance. Funding: This study was supported by grants from the Canadian Liver Foundation, Fonds de recherche du Québec–Santé (FRQS) AIDS and Infectious Disease Network (Réseau SIDA-MI), and the Canadian Network on Hepatitis C (CanHepC). CanHepC is funded by a joint initiative from the Canadian Institutes of Health Research (CIHR) (NHC-142832) and the Public Health Agency of Canada. M.F.M. received fellowships from the Université de Montréal, Bourse Gabriel Marquis, and the FRQS. T.F. received doctoral fellowships from CIHR and CanHepC. S.T. holds the Roger-Des-Groseillers Chair in hepatobiliary and pancreatic oncological surgery, Université de Montréal.

Author contributions: M.F.M. designed, performed experiments, and analyzed data. T.F. designed experiments. A.C-B. provided technical guidance. G.S. performed all the pathological assessment of the patient participants and provided input on all the pathological aspects. L.M. performed H&E staining, optimized, and performed image acquisition. M.N.A. performed the PSR stain and provided valuable technical input. N.B. contributed to the image analysis. S.T. is the principal investigator for the HBP biobank and is responsible for overseeing the overall operation of the biobank. He also provided invaluable input on all aspects of the project and its clinical implications. M.F.M, T.F., and N.H.S. conceptualized and designed the study. N.H.S. supervised the work and obtained funding. M.F.M., T.F., A.C-B, and N.H.S. wrote the manuscript. All authors reviewed and approved the manuscript.

#### **DISCLOSURES:**

The authors declare no conflicts of interest.

#### **REFERENCES:**

1. Greten, F. R., Grivennikov, S. I. Inflammation and Cancer: Triggers, Mechanisms, and Consequences. *Immunity*. **51** (1), 27–41 (2019).
2. Pages, F. et al. International validation of the consensus Immunoscore for the classification of colon cancer: a prognostic and accuracy study. *Lancet*. **391** (10135), 2128–2139 (2018).
3. Binnewies, M. et al. Understanding the tumor immune microenvironment (TIME) for effective therapy. *Nature Medicine*. **24** (5), 541–550 (2018).
4. Taube, J. M. et al. Implications of the tumor immune microenvironment for staging and therapeutics. *Modern Pathology: an official journal of the United States and Canadian Academy of Pathology, Inc.* **31** (2), 214–234 (2018).
5. Bindea, G. et al. Spatiotemporal dynamics of intratumoral immune cells reveal the immune landscape in human cancer. *Immunity*. **39** (4), 782–795 (2013).
6. Galon, J. et al. Towards the introduction of the 'Immunoscore' in the classification of

837 malignant tumours. *The Journal of Pathology*. **232** (2), 199–209 (2014).

838 7. Finotello, F., Eduati, F. Multi-Omics Profiling of the Tumor Microenvironment: Paving the  
839 Way to Precision Immuno-Oncology. *Frontiers in Oncology*. **8**, 430 (2018).

840 8. Gerner, M. Y., Kastenmuller, W., Ifrim, I., Kabat, J., Germain, R. N. Histo-cytometry: a  
841 method for highly multiplex quantitative tissue imaging analysis applied to dendritic cell subset  
842 microanatomy in lymph nodes. *Immunity*. **37** (2), 364–376 (2012).

843 9. Giesen, C. et al. Highly multiplexed imaging of tumor tissues with subcellular resolution  
844 by mass cytometry. *Nature Methods*. **11** (4), 417–422 (2014).

845 10. Porta Siegel, T. et al. Mass Spectrometry Imaging and Integration with Other Imaging  
846 Modalities for Greater Molecular Understanding of Biological Tissues. *Molecular Imaging and*  
847 *Biology : MIB: the official publication of the Academy of Molecular Imaging*. **20** (6), 888–901  
848 (2018).

849 11. Buchberger, A. R., DeLaney, K., Johnson, J., Li, L. Mass Spectrometry Imaging: A Review of  
850 Emerging Advancements and Future Insights. *Analytical Chemistry*. **90** (1), 240–265 (2018).

851 12. Pirici, D. et al. Antibody elution method for multiple immunohistochemistry on primary  
852 antibodies raised in the same species and of the same subtype. *Journal of Histochemistry and*  
853 *Cytochemistry*. **57** (6), 567–575 (2009).

854 13. Gendusa, R., Scalia, C. R., Buscone, S., Cattoretti, G. Elution of High-affinity (>10<sup>-9</sup> KD)  
855 Antibodies from Tissue Sections: Clues to the Molecular Mechanism and Use in Sequential  
856 Immunostaining. *Journal of Histochemistry and Cytochemistry*. **62** (7), 519–531 (2014).

857 14. van der Loos, C. M. Multiple immunoenzyme staining: methods and visualizations for the  
858 observation with spectral imaging. *Journal of Histochemistry and Cytochemistry*. **56** (4), 313–328  
859 (2008).

860 15. Stack, E. C., Wang, C., Roman, K. A., Hoyt, C. C. Multiplexed immunohistochemistry,  
861 imaging, and quantitation: a review, with an assessment of Tyramide signal amplification,  
862 multispectral imaging and multiplex analysis. *Methods*. **70** (1), 46–58 (2014).

863 16. Toth, Z. E., Mezey, E. Simultaneous visualization of multiple antigens with tyramide signal  
864 amplification using antibodies from the same species. *Journal of Histochemistry and*  
865 *Cytochemistry*. **55** (6), 545–554 (2007).

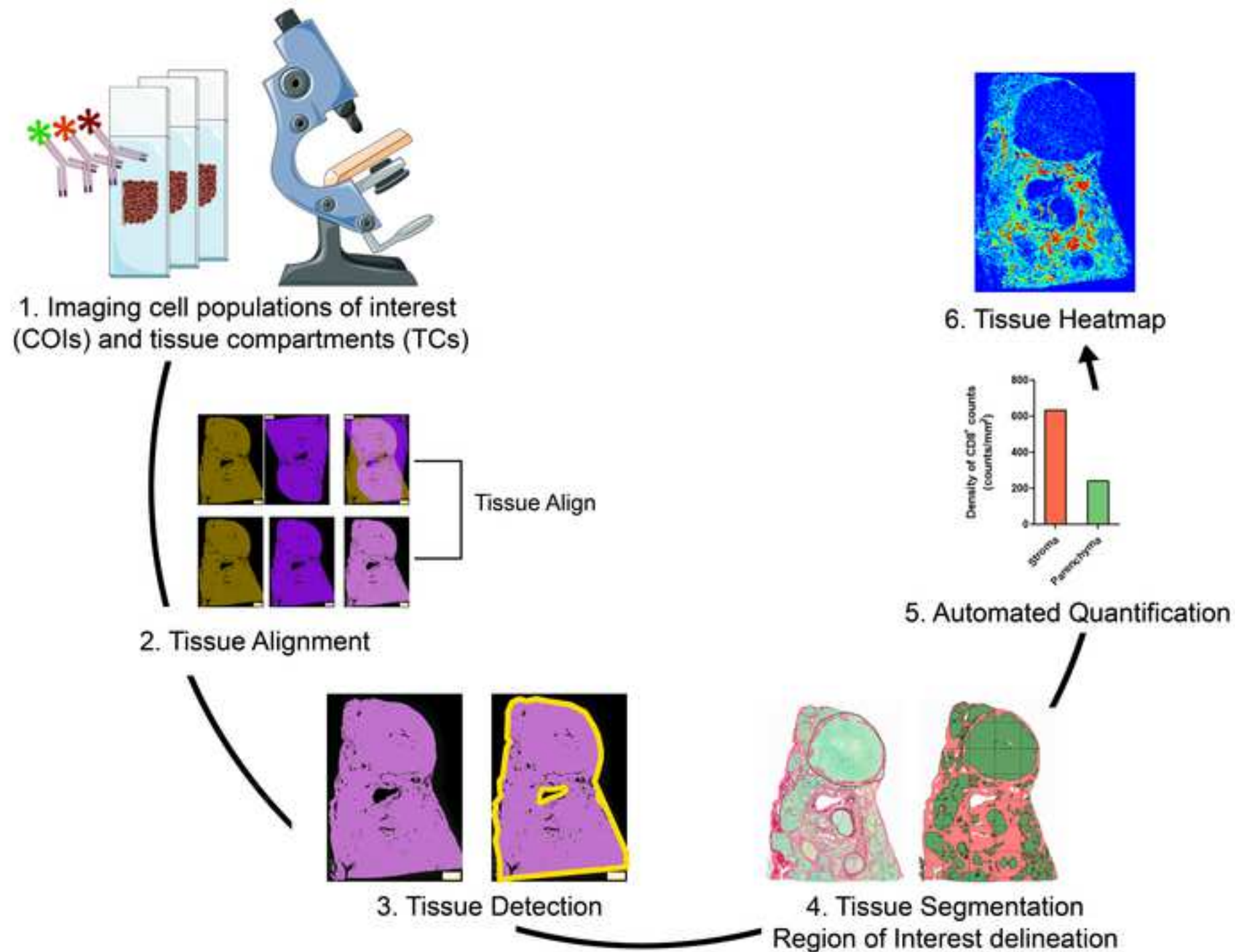
866 17. Robertson, D., Savage, K., Reis-Filho, J. S., Isacke, C. M. Multiple immunofluorescence  
867 labeling of formalin-fixed paraffin-embedded (FFPE) tissue. *BMC Cell Biology*. **9**, 13 (2008).

868 18. Segnani, C. et al. Histochemical Detection of Collagen Fibers by Sirius Red/Fast Green Is  
869 More Sensitive than van Gieson or Sirius Red Alone in Normal and Inflamed Rat Colon. *PloS One*.  
870 **10** (12), e0144630 (2015).

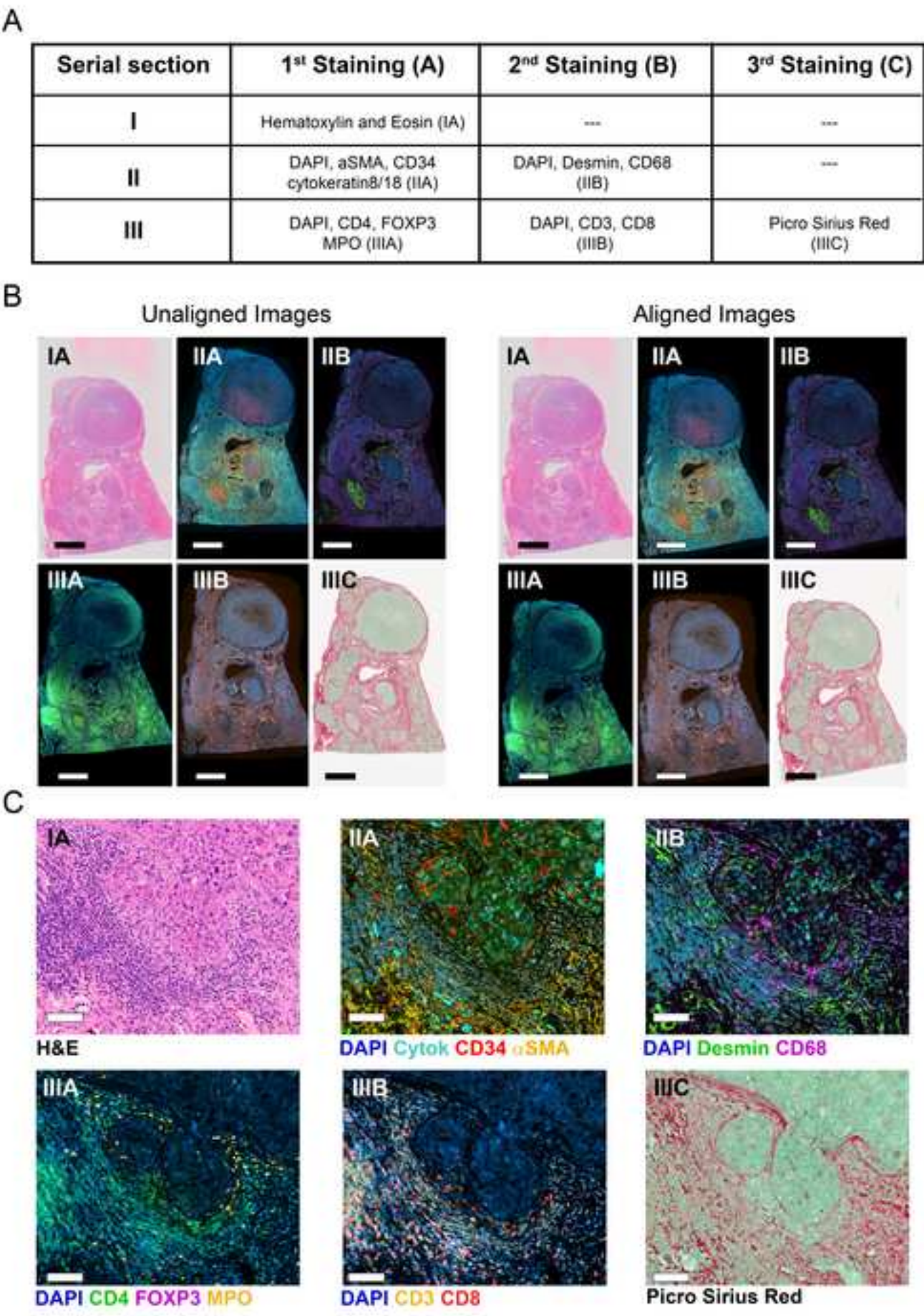
871 19. Bolognesi, M. M. et al. Multiplex Staining by Sequential Immunostaining and Antibody  
872 Removal on Routine Tissue Sections. *Journal of Histochemistry and Cytochemistry*. **65** (8), 431–  
873 444 (2017).

874



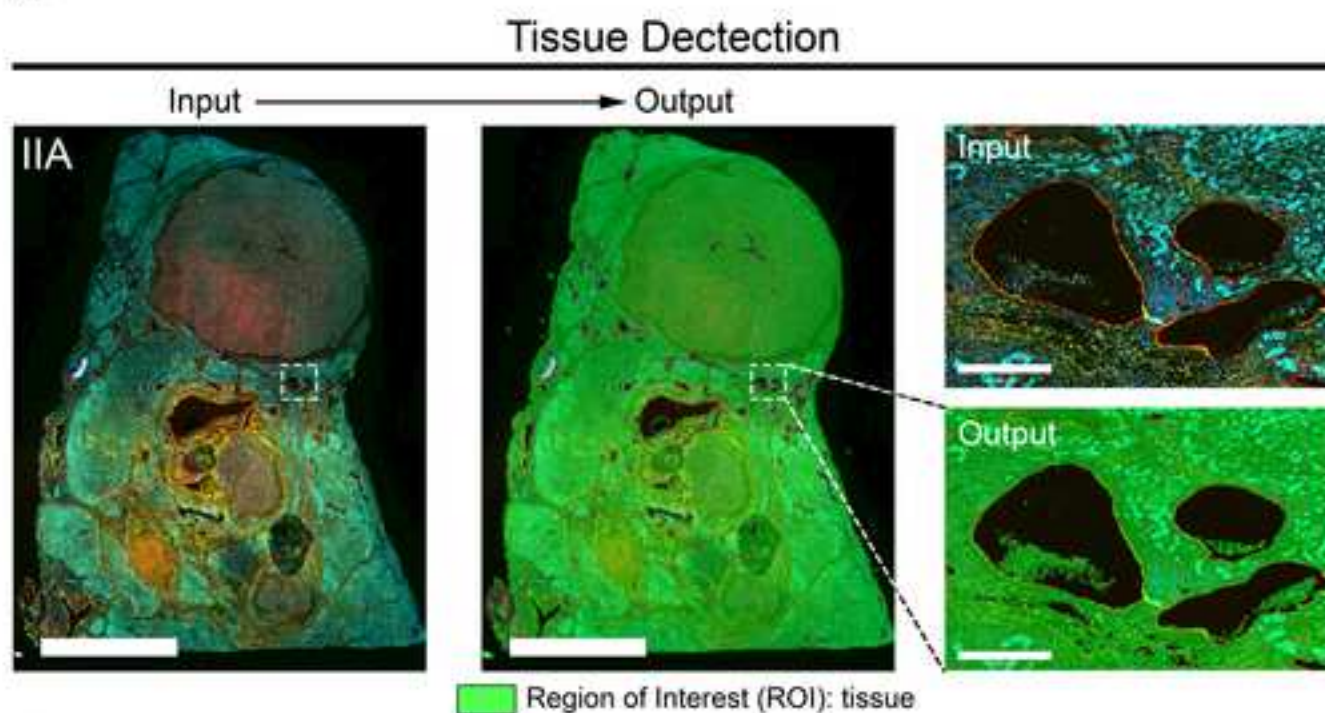








A



B

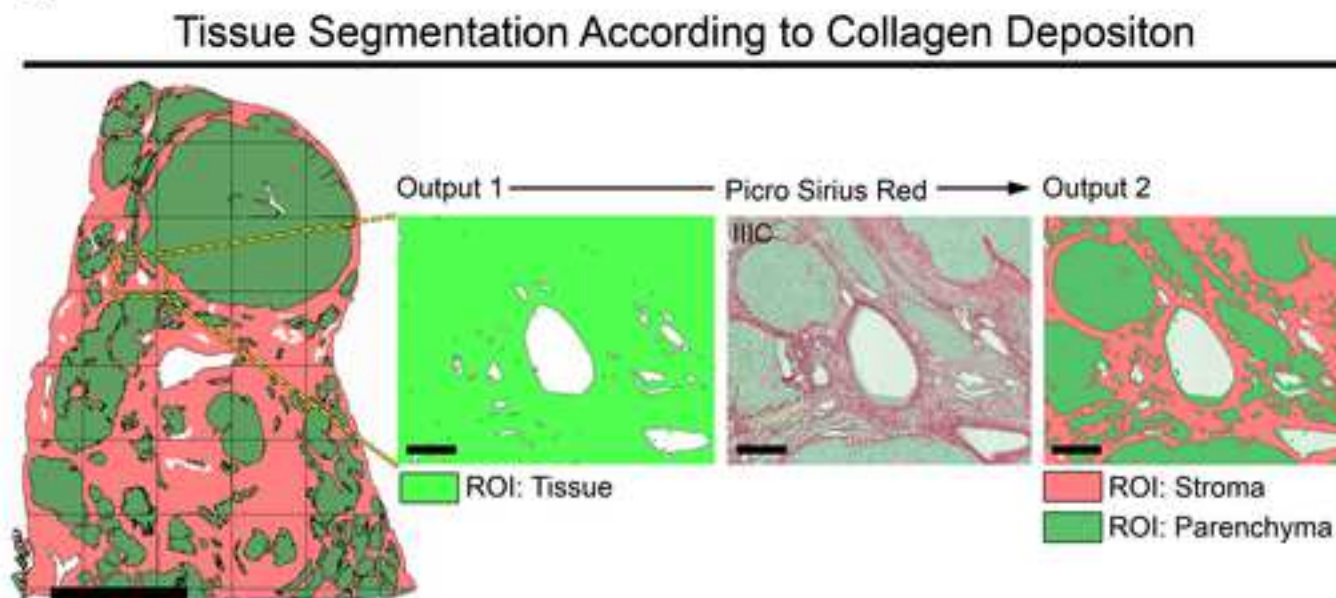


Figure 4

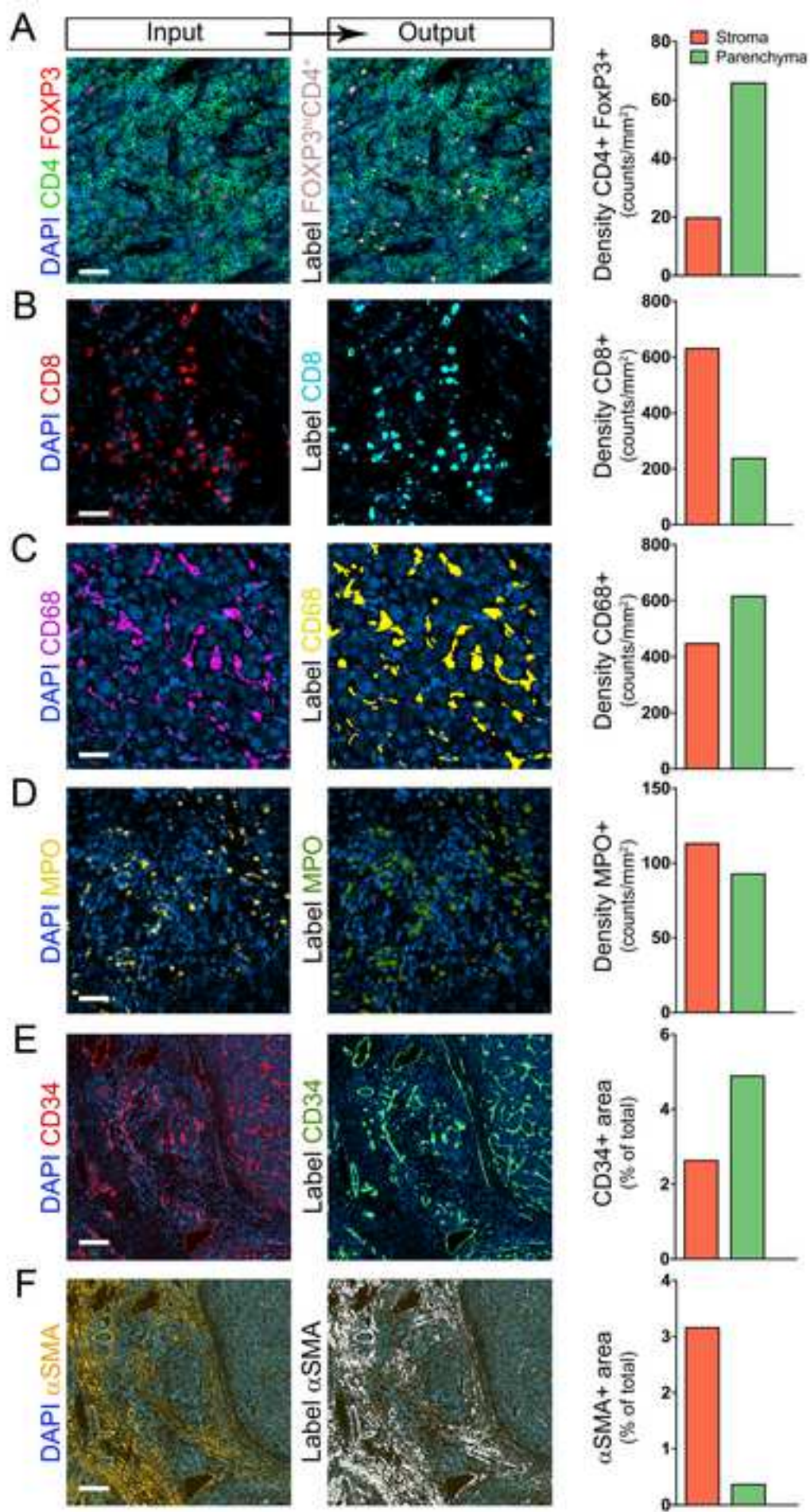
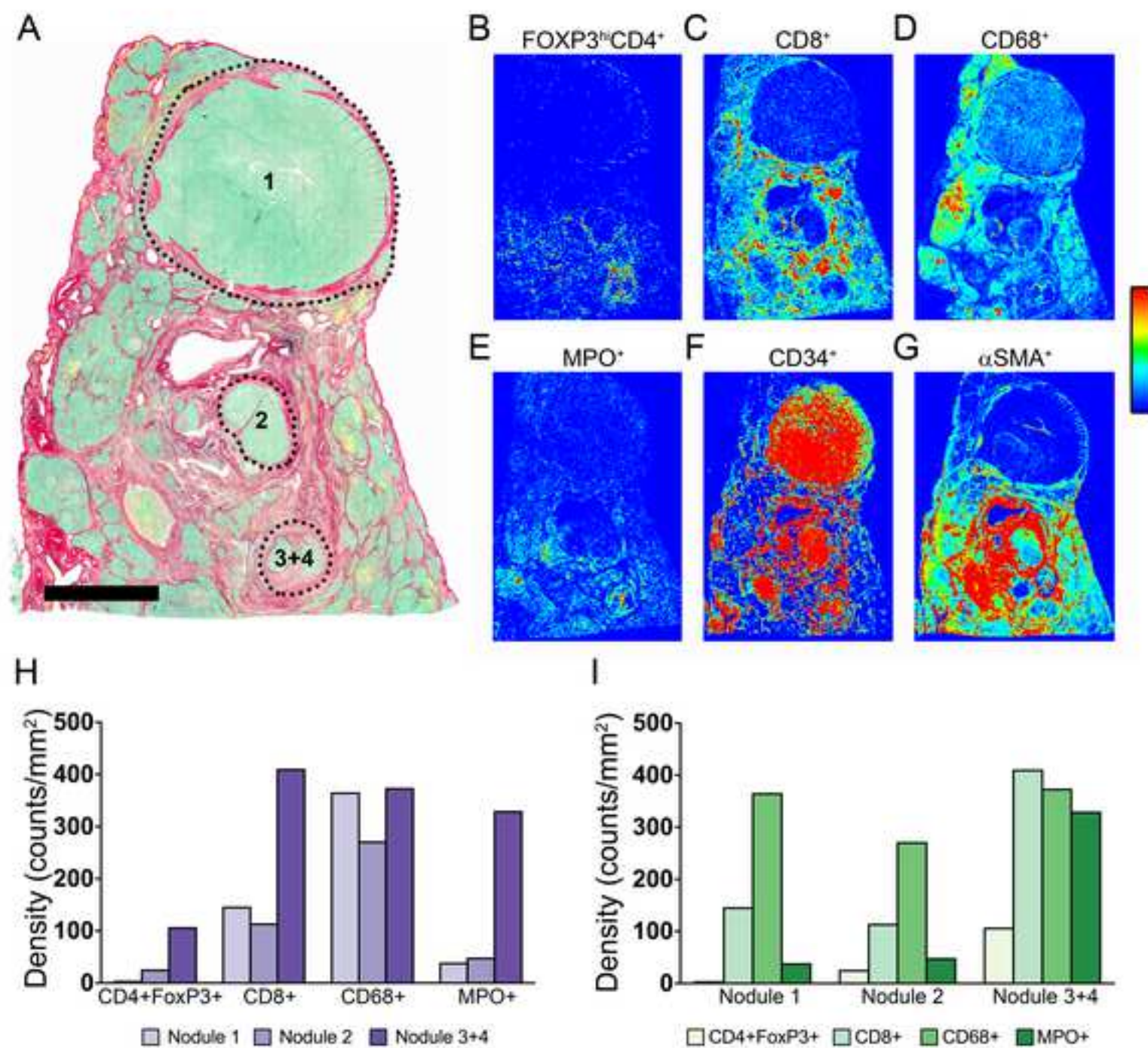




Figure 5

[Click here to access/download;Figure;Figure 5.tif](#)



APP	Purpose	Classification Method
1	Tissue detection	Threshold
2	Tissue Segmentation	Decision Forest
3	To locate and quantify CD4+ FoxP3+ cells	Threshold
4	To locate and quantify CD8+ cells	Threshold
5	To locate and quantify CD68+ cells	Threshold
6	To locate and quantify MPO+ cells	Threshold

7	To locate and quantify $\alpha$ SMA+ area	Threshold
8	To locate and quantify CD34+ area	Threshold
9	Create tissue heatmaps for a given cell population	Object Heatmap
10	Quantify colocalization between $\alpha$ SMA and Desmin	Threshold

Classification Features (pixel value)	Post-Processing Steps	Output Variables
Channel DAPI (150)	<ul style="list-style-type: none"> <li>Label objects with colocalized above-threshold values for the 3 channels</li> </ul>	<ul style="list-style-type: none"> <li>ROI Tissue</li> </ul>
Channel FITC/A488 (120)	<ul style="list-style-type: none"> <li>Close positive object 5 pixels</li> </ul>	<ul style="list-style-type: none"> <li>Tissue Area</li> </ul>
Channel TRITC/A568 (40)	<ul style="list-style-type: none"> <li>Create ROI Tissue</li> </ul>	
RGB-R median	<ul style="list-style-type: none"> <li>Fill holes</li> </ul>	<ul style="list-style-type: none"> <li>ROI Stroma</li> </ul>
RGB-G median	<ul style="list-style-type: none"> <li>Create ROI Stroma</li> </ul>	<ul style="list-style-type: none"> <li>Stroma Area</li> </ul>
RGB-B median	<ul style="list-style-type: none"> <li>Create ROI Parenchyma</li> </ul>	<ul style="list-style-type: none"> <li>ROI Parenchyma</li> </ul>
IHS-S median		<ul style="list-style-type: none"> <li>Parenchyma Area</li> </ul>
H&E Eosin median		
Channel DAPI (>600)	<ul style="list-style-type: none"> <li>Label objects with colocalization of DAPI and Cy5/A647, surrounded by FITC/A488 signal</li> </ul>	<ul style="list-style-type: none"> <li>Counts and density of CD4+FoxP3+ cells in ROIs Stroma and Parenchyma</li> </ul>
Channel FITC/A488 poly smoothing (>850)	<ul style="list-style-type: none"> <li>Clear objects smaller than <math>7 \mu\text{m}^2</math></li> </ul>	<ul style="list-style-type: none"> <li>Coordinates of individual CD4+FoxP3+ cells</li> </ul>
Channel Cy5/A647 (>800)		
Channel DAPI (<1200)	<ul style="list-style-type: none"> <li>Clear positive objects smaller than <math>15 \mu\text{m}^2</math></li> </ul>	<ul style="list-style-type: none"> <li>Counts and density of CD8+ cells in ROIs Stroma and Parenchyma</li> </ul>
Channel Cy5/A647 median (>80)	<ul style="list-style-type: none"> <li>Close positive objects 2 pixels</li> <li>Separate objects</li> </ul>	<ul style="list-style-type: none"> <li>Coordinates of individual cells</li> </ul>
Channel FITC/A488 (>200)	<ul style="list-style-type: none"> <li>Clear positive objects smaller than <math>20 \mu\text{m}^2</math></li> <li>Dilate positive objects 3 pixels</li> <li>Separate objects</li> </ul>	<ul style="list-style-type: none"> <li>Counts and density of CD68+ cells in ROIs Stroma and Parenchyma</li> <li>Coordinates of individual CD68+ cells</li> </ul>
Channel DAPI (>400)	<ul style="list-style-type: none"> <li>Clear objects smaller than <math>5 \mu\text{m}^2</math></li> </ul>	<ul style="list-style-type: none"> <li>Counts and density of MPO+ cells in ROIs Stroma and Parenchyma.</li> </ul>
Channel TRITC/A568 (900-4000)	<ul style="list-style-type: none"> <li>Dilate 3 pixels positive objects</li> <li>Separate objects</li> </ul>	<ul style="list-style-type: none"> <li>Coordinates of individual MPO+ cells.</li> </ul>

Channel TRITC/CF568 (>1050)	<ul style="list-style-type: none"> <li>○ Clear positive objects smaller than <math>25\ \mu\text{m}^2</math></li> <li>○ Dilate 3 pixels positive objects</li> </ul>	<ul style="list-style-type: none"> <li>○ Counts and density of <math>\alpha\text{SMA}^+</math> area in ROIs Stroma and Parenchyma</li> <li>○ Coordinates of <math>\alpha\text{SMA}^+</math> pixels</li> </ul>
Channel DAPI (<5000)	<ul style="list-style-type: none"> <li>○ Clear positive objects smaller than <math>25\ \mu\text{m}^2</math></li> </ul>	<ul style="list-style-type: none"> <li>○ Counts and density of <math>\text{CD}34^+</math> area in ROIs Stroma and Parenchyma</li> </ul>
Channel Cy5/A647 median (>120)	<ul style="list-style-type: none"> <li>○ Dilate 3 pixels positive objects</li> </ul>	<ul style="list-style-type: none"> <li>○ Coordinates of <math>\text{CD}34^+</math> pixels</li> </ul>
Object Heatmap		<ul style="list-style-type: none"> <li>○ Heatmap</li> </ul>
Drawing radius $50\ \mu\text{m}$	---	
Channel TRITC (CF568) (>1050)	<ul style="list-style-type: none"> <li>○ Label objects with above threshold values for TRITC (CF568)</li> </ul>	<ul style="list-style-type: none"> <li>○ Quantify colocalized expression of <math>\alpha\text{SMA}</math> and Desmin</li> </ul>
Channel Cy5 (A647) (>1000)	<ul style="list-style-type: none"> <li>○ Label objects with above threshold values for Cy5 (A647)</li> <li>○ Label objects with colocalization of above threshold values for TRITC (CF568) and Cy5 (A647)</li> <li>○ Clear positive objects smaller than <math>25\ \mu\text{m}^2</math></li> </ul>	

Section/Staining	Primary Antibody
Section II/1 <sup>st</sup> Staining	Mouse IgG2a anti-human αSMA
	Mouse IgG1 anti-human CD34
	Rabbit anti-human Cytokeratin 8/18
Section II/2 <sup>nd</sup> Staining	Rabbit anti-human Desmin
	Mouse anti-human CD68
Section III/1 <sup>st</sup> Staining	Mouse anti-human CD4
	Rabbit anti-human FoxP3
	Goat anti-human MPO
Section III/2 <sup>nd</sup> Staining	Rabbit anti-human CD3
	Mouse anti-human CD8



## Secondary Antibody

Goat anti-mouse IgG2a CF568

Rat anti-mouse IgG1 A647

Donkey anti-rabbit A488

Donkey anti-rabbit A647

Donkey anti-mouse DyLight 755

Donkey anti-mouse A488

Donkey anti-rabbit A647

Donkey anti-goat A568

Donkey anti-mouse DyLight 755

Donkey anti-rabbit A647





Name of Material/ Equipment
Antigen Retrieval Solution: Sodium Citrate Buffer (10 mM Sodium Citrate, 0.05% v/v Tween 20, pH 6.0)
Blocking Solution: 1 % BSA, 10 % filtered human serum, 10 % filtered donkey serum, 0.1 % Tween 20, and 0.3% Tri
Bovine serum albumin (BSA)
Coplin jars (EASYDIP SLIDE STAINING SYSTEM)
Cover slides
Direct Red 80
Donkey Serum
Ethanol 100%
Electric pressure cooker
Eosin
Fast Green FCF
FFPE section (4µm) slides
Glycine 0,1 M in PBS
Hematoxylin Stain Solution, Gil 1. Formulation, Regular Strength
Holder (EasyDip Staining Jar Holder)
Human Serum
Humidity chamber
Pap pen
PBS
PBS-Tween 20 (0.1% v/v)
Permout Mounting Media
Picric Acid 1.3 %
Picro-Sirius Red/Fast Green solution: Fast Green 0.1 % w/v + Sirius Red 0.2 % w/v in 1,3 % picric acid solution
Primary Antibody Anti-αSMA
Primary Antibody Anti-CD34
Primary Antibody Anti-Cytokeratin 8/18
Primary Antibody Anti-CD68
Primary Antibody Anti-Desmin
Primary Antibody Anti-CD4
Primary Antibody Anti-FoxP3
Primary Antibody Anti-MPO
Primary Antibody Anti-CD3
Primary Antibody Anti-CD8
Secondary Antibody Donkey anti-mouse A488
Secondary Antibody Donkey anti-Rabbit A488
Secondary Antibody Donkey anti-goat A568
Secondary Antibody Donkey anti-rabbit A647
Secondary Antibody Rat anti-mouse IgG1 A647
Secondary Antibody Goat anti-mouse IgG2a CF568
Secondary Antibody Donkey anti-mouse DyLight 755
Secondary Antibody Donkey anti-rabbit DyLight 755
SDS
Shandon multi-program robotic slide stainer

Shandon Xylene Substitute,
Shaking water bath
SlowFade Gold antifade reagent with DAPI
Sodium Citrate Dihydrate
Stripping Buffer: mix 20 ml 10% w/v SDS with 12.5 ml 0.5 M Tris-HCl (pH 6.8), and 67.5 ml ultra-pure water. Under
Triton X-100
Tris-HCl
Tween 20
VIS Software
Whole slide scanner Olympus BX61VS
Xylene
Xylene : Ethanol solution (1:1 v/v)
2-mercaptoethanol

Company	Catalog Number
iton in PBS	
Multicell	800-095-EG
Newcomersupply	5300KIT
Fisherbrand	12-545E 22*50
Sigma Aldrich	365548
Sigma Aldrich	D9663
Salton	
Leica Biosystems	3801600
Sigma Aldrich	F7252
Ricca Chemical Company	3535-32
Newcomersupply	5300RK
Gemini	22210
Millipore Sigma	Z670138-1EA
abcam	ab2601
Fisher Chemical	SP15-500
Sigma Aldrich	P6744
Mouse IgG2a 1A4	Sigma A2547
Mouse IgG1 HPCA1/763	Novus Biologicals NBP2-44568
Rabbit EP17/EP30	Agilent IR09461-2
Mouse KP1	Abcam ab955
Rabbit Polyclonal	Invitrogen PA5-16705
Mouse N1UG0	Affymetrix 14-2444
Rabbit 1054C	R & D MAB8214
Goat Polyclonal	R & D Systems AF3667
Rabbit SP7	Abcam ab16669
Mouse C8/144B	Invitrogen 14-0085-80
Polyclonal	Invitrogen A-21202
Polyclonal	Invitrogen A-21206
Polyclonal	Invitrogen A-11057
Polyclonal	Invitrogen A-31573
RMG1-1	Biolegend 406618
Polyclonal	Sigma Aldrich SAB4600315
Polyclonal	Invitrogen SA5-10171
Polyclonal	Invitrogen SA5-10043
BioShop	SDS001,500
LabX	11384903

Thermo Fisher Scientific	CA89413-336
Invitrogen	S36938
Millipore Sigma	1545801
In a fume hood, add 800 uL of 2-mercapto ethanol (114,4 mM final concentration)	
Sigma Aldrich	T8787-50ML
BioShop	77-86-1
Fisher Scientific	BP337-500
Visiopharm	
Olympus	
Sigma Aldrich	214736-4L
Sigma	M6250

Comments/Description
CAUTION, eye irritation
CAUTION, harmful by inhalation, ingestion and skin absorption
CAUTION, skin and eye irritation
Dilution 1/100
Dilution 1/250
Ready to use
Dilution 1/200
Dilution 1/200
Dilution 1/250
Dilution 1/100
Dilution 1/250
Dilution 1/200
Dilution 1/200
Dilution 1/500
Dilution 1/500
Dilution 1/500
Dilution 1/500
Dilution 1/500
Dilution 1/500
Dilution 1/500
Dilution 1/500
CAUTION, oral skin and eye toxicity



CAUTION, Flammable, skin and eye irritation, Harmful when inhaled

CAUTION, eye irritation

Microscope: Olympus Slide Scanner BX61VS, 5 slides scanner, motorized stage, autofocus. Camera: Ligt

CAUTION, Flammable, skin and eye irritation, Harmful when inhaled

CAUTION, harmful by ingestion, inhalation, fatal if sking absortion. Eye irritation. Use fume hood



htsource: Xcite-120. Filters: BrightLine® Sedat filter set (# LED-DA/FI/TR/Cy5-4X4M-B-000, Semrock)



November 17, 2019

**Dr. Alisha DSouza**

Senior Editor, Immunology and Infection  
Editorial Department  
JoVE  
1 Alewife Center, Suite 200  
Cambridge, MA 02140  
USA

**Subject: Revised manuscript submission JoVE60740**

Dear Dr. DSouza,

On behalf of myself and the co-authors I would like to thank you and the reviewers for the favorable review of our manuscript, JoVE60740: **“Strategy for visualization, quantification, and mapping of immune cell populations in the tumor microenvironment”**.

We have significantly addressed the additional points you raised in your last review

We believe that this novel methodology findings will be of great interest to the field of Immunology, Infection and Cancer, especially at institutes with limited budget.

I thank you in advance for this invitation and I look forward to a favorable response from you on behalf of JoVE.

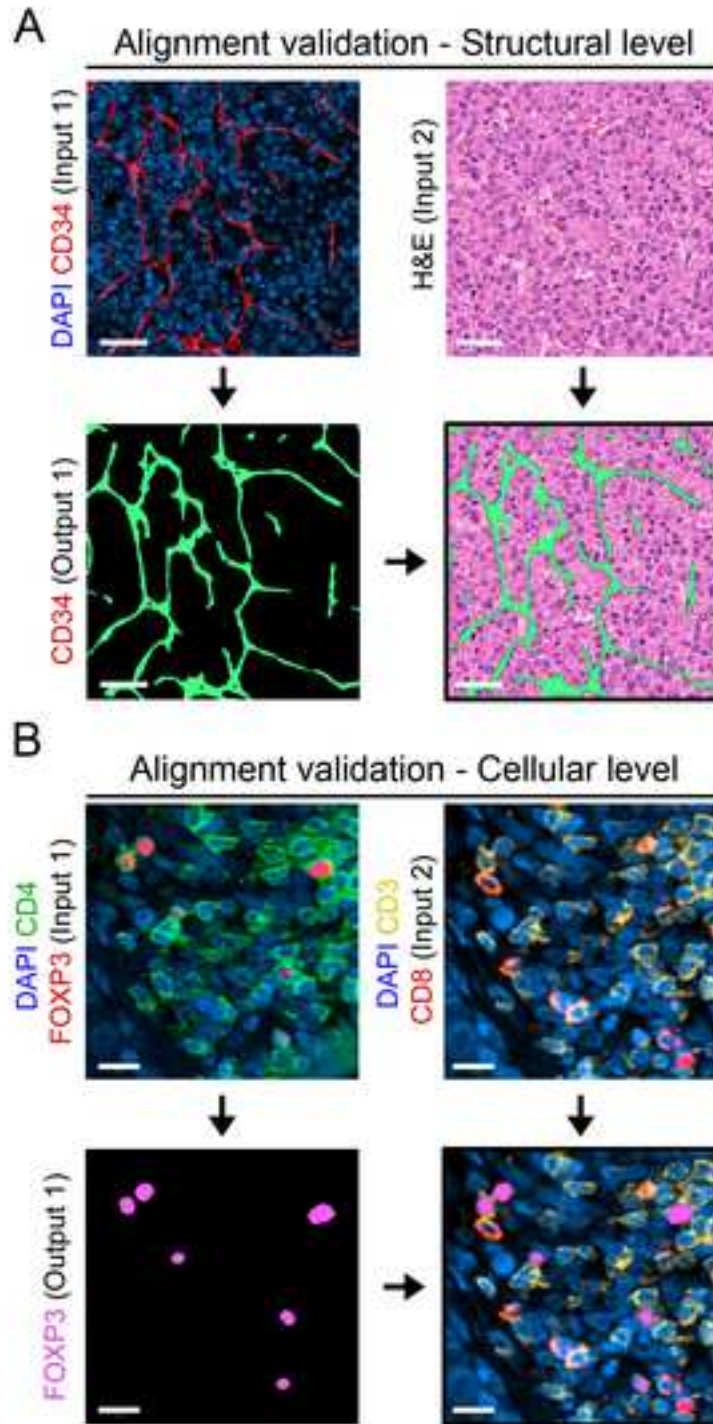
Sincerely,

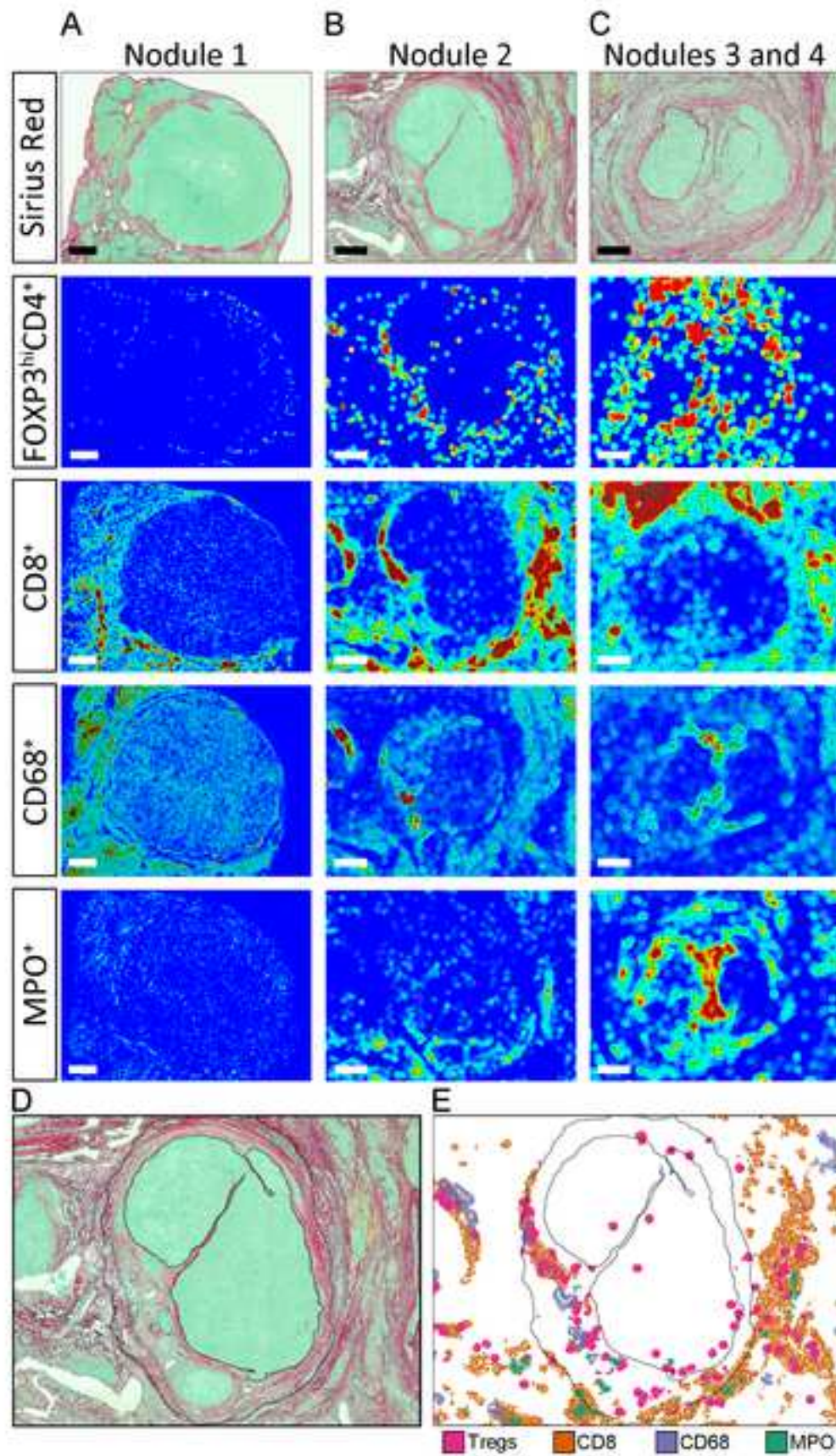
**Naglaa Shoukry, B. Pharm, Ph.D.**

Professor, Department of Medicine, University of Montreal  
Director, Canadian Network on Hepatitis C (CanHepC)

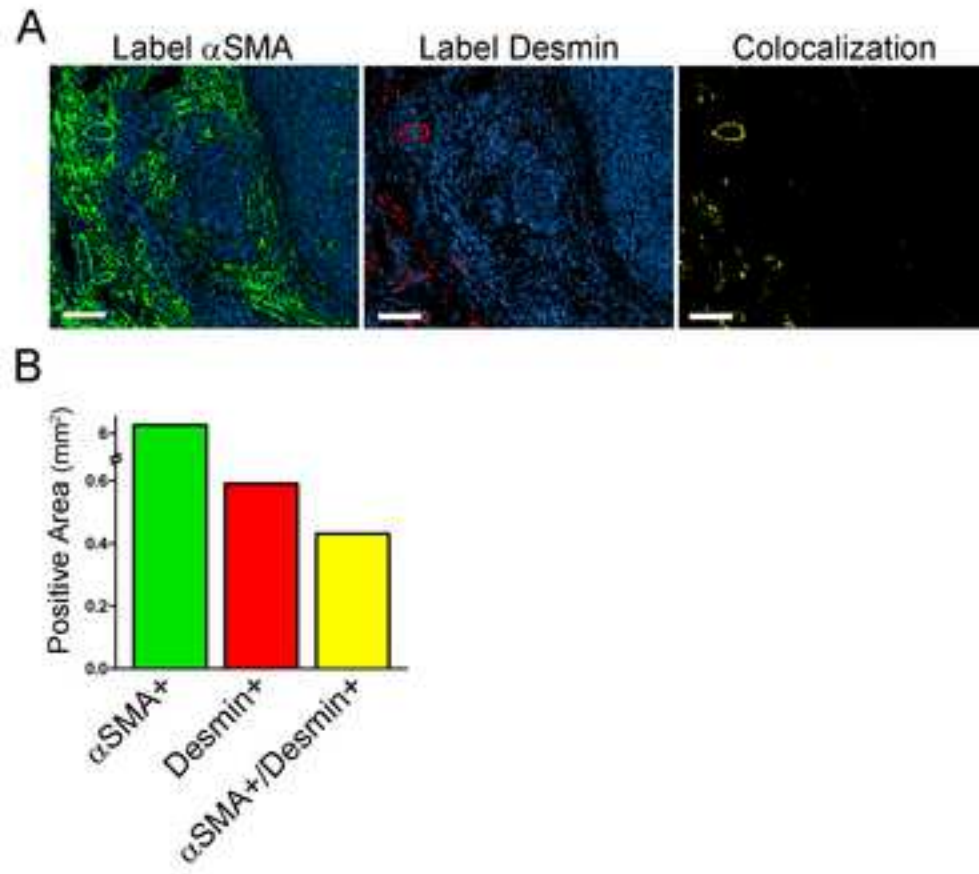
Mailing address:

Centre de Recherche du CHUM  
Tour Viger, Local R09.414  
900 rue St-Denis  
Montréal, QC H2X 0A9  
CANADA









## ARTICLE AND VIDEO LICENSE AGREEMENT

Title of Article:	Strategy for visualization, quantification, and mapping of immune cell populations in the tumor microenvironment
Author(s):	M Flores-Molina, T Fabre, A Cleret-Buhot, G Soucy, L Meunier, M N Abdelnabi, N Belforte, S Turcotte, NH Shoukry

Item 1: The Author elects to have the Materials be made available (as described at <http://www.jove.com/publish>) via:



Standard Access



Open Access

Item 2: Please select one of the following items:



The Author is **NOT** a United States government employee.



The Author is a United States government employee and the Materials were prepared in the course of his or her duties as a United States government employee.



The Author is a United States government employee but the Materials were NOT prepared in the course of his or her duties as a United States government employee.

### ARTICLE AND VIDEO LICENSE AGREEMENT

1. **Defined Terms.** As used in this Article and Video License Agreement, the following terms shall have the following meanings: “**Agreement**” means this Article and Video License Agreement; “**Article**” means the article specified on the last page of this Agreement, including any associated materials such as texts, figures, tables, artwork, abstracts, or summaries contained therein; “**Author**” means the author who is a signatory to this Agreement; “**Collective Work**” means a work, such as a periodical issue, anthology or encyclopedia, in which the Materials in their entirety in unmodified form, along with a number of other contributions, constituting separate and independent works in themselves, are assembled into a collective whole; “**CRC License**” means the Creative Commons Attribution-Non Commercial-No Derivs 3.0 Unported Agreement, the terms and conditions of which can be found at: <http://creativecommons.org/licenses/by-nc-nd/3.0/legalcode>; “**Derivative Work**” means a work based upon the Materials or upon the Materials and other pre-existing works, such as a translation, musical arrangement, dramatization, fictionalization, motion picture version, sound recording, art reproduction, abridgment, condensation, or any other form in which the Materials may be recast, transformed, or adapted; “**Institution**” means the institution, listed on the last page of this Agreement, by which the Author was employed at the time of the creation of the Materials; “**JoVE**” means MyJoVE Corporation, a Massachusetts corporation and the publisher of The Journal of Visualized Experiments; “**Materials**” means the Article and / or the Video; “**Parties**” means the Author and JoVE; “**Video**” means any video(s) made by the Author, alone or in conjunction with any other parties, or by JoVE or its affiliates or agents, individually or in collaboration with the Author or any other parties, incorporating all or any portion

of the Article, and in which the Author may or may not appear.

2. **Background.** The Author, who is the author of the Article, in order to ensure the dissemination and protection of the Article, desires to have the JoVE publish the Article and create and transmit videos based on the Article. In furtherance of such goals, the Parties desire to memorialize in this Agreement the respective rights of each Party in and to the Article and the Video.

3. **Grant of Rights in Article.** In consideration of JoVE agreeing to publish the Article, the Author hereby grants to JoVE, subject to **Sections 4** and **7** below, the exclusive, royalty-free, perpetual (for the full term of copyright in the Article, including any extensions thereto) license (a) to publish, reproduce, distribute, display and store the Article in all forms, formats and media whether now known or hereafter developed (including without limitation in print, digital and electronic form) throughout the world, (b) to translate the Article into other languages, create adaptations, summaries or extracts of the Article or other Derivative Works (including, without limitation, the Video) or Collective Works based on all or any portion of the Article and exercise all of the rights set forth in (a) above in such translations, adaptations, summaries, extracts, Derivative Works or Collective Works and (c) to license others to do any or all of the above. The foregoing rights may be exercised in all media and formats, whether now known or hereafter devised, and include the right to make such modifications as are technically necessary to exercise the rights in other media and formats. If the “Open Access” box has been checked in **Item 1** above, JoVE and the Author hereby grant to the public all such rights in the Article as provided in, but subject to all limitations and requirements set forth in, the CRC License.

612542.6 For questions, please contact us at [submissions@jove.com](mailto:submissions@jove.com) or +1.617.945.9051.



## ARTICLE AND VIDEO LICENSE AGREEMENT

4. **Retention of Rights in Article.** Notwithstanding the exclusive license granted to JoVE in **Section 3** above, the Author shall, with respect to the Article, retain the non-exclusive right to use all or part of the Article for the non-commercial purpose of giving lectures, presentations or teaching classes, and to post a copy of the Article on the Institution's website or the Author's personal website, in each case provided that a link to the Article on the JoVE website is provided and notice of JoVE's copyright in the Article is included. All non-copyright intellectual property rights in and to the Article, such as patent rights, shall remain with the Author.

5. **Grant of Rights in Video – Standard Access.** This **Section 5** applies if the "Standard Access" box has been checked in **Item 1** above or if no box has been checked in **Item 1** above. In consideration of JoVE agreeing to produce, display or otherwise assist with the Video, the Author hereby acknowledges and agrees that, Subject to **Section 7** below, JoVE is and shall be the sole and exclusive owner of all rights of any nature, including, without limitation, all copyrights, in and to the Video. To the extent that, by law, the Author is deemed, now or at any time in the future, to have any rights of any nature in or to the Video, the Author hereby disclaims all such rights and transfers all such rights to JoVE.

6. **Grant of Rights in Video – Open Access.** This **Section 6** applies only if the "Open Access" box has been checked in **Item 1** above. In consideration of JoVE agreeing to produce, display or otherwise assist with the Video, the Author hereby grants to JoVE, subject to **Section 7** below, the exclusive, royalty-free, perpetual (for the full term of copyright in the Article, including any extensions thereto) license (a) to publish, reproduce, distribute, display and store the Video in all forms, formats and media whether now known or hereafter developed (including without limitation in print, digital and electronic form) throughout the world, (b) to translate the Video into other languages, create adaptations, summaries or extracts of the Video or other Derivative Works or Collective Works based on all or any portion of the Video and exercise all of the rights set forth in (a) above in such translations, adaptations, summaries, extracts, Derivative Works or Collective Works and (c) to license others to do any or all of the above. The foregoing rights may be exercised in all media and formats, whether now known or hereafter devised, and include the right to make such modifications as are technically necessary to exercise the rights in other media and formats. For any Video to which this **Section 6** is applicable, JoVE and the Author hereby grant to the public all such rights in the Video as provided in, but subject to all limitations and requirements set forth in, the CRC License.

7. **Government Employees.** If the Author is a United States government employee and the Article was prepared in the course of his or her duties as a United States government employee, as indicated in **Item 2** above, and any of the licenses or grants granted by the Author hereunder exceed the scope of the 17 U.S.C. 403, then the rights granted hereunder shall be limited to the maximum

rights permitted under such statute. In such case, all provisions contained herein that are not in conflict with such statute shall remain in full force and effect, and all provisions contained herein that do so conflict shall be deemed to be amended so as to provide to JoVE the maximum rights permissible within such statute.

8. **Protection of the Work.** The Author(s) authorize JoVE to take steps in the Author(s) name and on their behalf if JoVE believes some third party could be infringing or might infringe the copyright of either the Author's Article and/or Video.

9. **Likeness, Privacy, Personality.** The Author hereby grants JoVE the right to use the Author's name, voice, likeness, picture, photograph, image, biography and performance in any way, commercial or otherwise, in connection with the Materials and the sale, promotion and distribution thereof. The Author hereby waives any and all rights he or she may have, relating to his or her appearance in the Video or otherwise relating to the Materials, under all applicable privacy, likeness, personality or similar laws.

10. **Author Warranties.** The Author represents and warrants that the Article is original, that it has not been published, that the copyright interest is owned by the Author (or, if more than one author is listed at the beginning of this Agreement, by such authors collectively) and has not been assigned, licensed, or otherwise transferred to any other party. The Author represents and warrants that the author(s) listed at the top of this Agreement are the only authors of the Materials. If more than one author is listed at the top of this Agreement and if any such author has not entered into a separate Article and Video License Agreement with JoVE relating to the Materials, the Author represents and warrants that the Author has been authorized by each of the other such authors to execute this Agreement on his or her behalf and to bind him or her with respect to the terms of this Agreement as if each of them had been a party hereto as an Author. The Author warrants that the use, reproduction, distribution, public or private performance or display, and/or modification of all or any portion of the Materials does not and will not violate, infringe and/or misappropriate the patent, trademark, intellectual property or other rights of any third party. The Author represents and warrants that it has and will continue to comply with all government, institutional and other regulations, including, without limitation all institutional, laboratory, hospital, ethical, human and animal treatment, privacy, and all other rules, regulations, laws, procedures or guidelines, applicable to the Materials, and that all research involving human and animal subjects has been approved by the Author's relevant institutional review board.

11. **JoVE Discretion.** If the Author requests the assistance of JoVE in producing the Video in the Author's facility, the Author shall ensure that the presence of JoVE employees, agents or independent contractors is in accordance with the relevant regulations of the Author's institution. If more than one author is listed at the beginning of this Agreement, JoVE may, in its sole

## ARTICLE AND VIDEO LICENSE AGREEMENT

discretion, elect not take any action with respect to the Article until such time as it has received complete, executed Article and Video License Agreements from each such author. JoVE reserves the right, in its absolute and sole discretion and without giving any reason therefore, to accept or decline any work submitted to JoVE. JoVE and its employees, agents and independent contractors shall have full, unfettered access to the facilities of the Author or of the Author's institution as necessary to make the Video, whether actually published or not. JoVE has sole discretion as to the method of making and publishing the Materials, including, without limitation, to all decisions regarding editing, lighting, filming, timing of publication, if any, length, quality, content and the like.

12. **Indemnification.** The Author agrees to indemnify JoVE and/or its successors and assigns from and against any and all claims, costs, and expenses, including attorney's fees, arising out of any breach of any warranty or other representations contained herein. The Author further agrees to indemnify and hold harmless JoVE from and against any and all claims, costs, and expenses, including attorney's fees, resulting from the breach by the Author of any representation or warranty contained herein or from allegations or instances of violation of intellectual property rights, damage to the Author's or the Author's institution's facilities, fraud, libel, defamation, research, equipment, experiments, property damage, personal injury, violations of institutional, laboratory, hospital, ethical, human and animal treatment, privacy or other rules, regulations, laws, procedures or guidelines, liabilities and other losses or damages related in any way to the submission of work to JoVE, making of videos by JoVE, or publication in JoVE or elsewhere by JoVE. The Author shall be responsible for, and shall hold JoVE harmless from, damages caused by lack of sterilization, lack of cleanliness or by contamination due to


the making of a video by JoVE its employees, agents or independent contractors. All sterilization, cleanliness or decontamination procedures shall be solely the responsibility of the Author and shall be undertaken at the Author's expense. All indemnifications provided herein shall include JoVE's attorney's fees and costs related to said losses or damages. Such indemnification and holding harmless shall include such losses or damages incurred by, or in connection with, acts or omissions of JoVE, its employees, agents or independent contractors.

13. **Fees.** To cover the cost incurred for publication, JoVE must receive payment before production and publication of the Materials. Payment is due in 21 days of invoice. Should the Materials not be published due to an editorial or production decision, these funds will be returned to the Author. Withdrawal by the Author of any submitted Materials after final peer review approval will result in a US\$1,200 fee to cover pre-production expenses incurred by JoVE. If payment is not received by the completion of filming, production and publication of the Materials will be suspended until payment is received.

14. **Transfer, Governing Law.** This Agreement may be assigned by JoVE and shall inure to the benefits of any of JoVE's successors and assignees. This Agreement shall be governed and construed by the internal laws of the Commonwealth of Massachusetts without giving effect to any conflict of law provision thereunder. This Agreement may be executed in counterparts, each of which shall be deemed an original, but all of which together shall be deemed to be one and the same agreement. A signed copy of this Agreement delivered by facsimile, e-mail or other means of electronic transmission shall be deemed to have the same legal effect as delivery of an original signed copy of this Agreement.

A signed copy of this document must be sent with all new submissions. Only one Agreement is required per submission.

### CORRESPONDING AUTHOR

Name:	Naglaa H. Shoukry	
Department:	Department of Medicine	
Institution:	Centre de Recherche du CHUM (CRCHUM)	
Title:	Professor	
Signature:		Date: 08/30/2019

Please submit a **signed** and **dated** copy of this license by one of the following three methods:

1. Upload an electronic version on the JoVE submission site
2. Fax the document to +1.866.381.2236
3. Mail the document to JoVE / Attn: JoVE Editorial / 1 Alewife Center #200 / Cambridge, MA 02140



612542.6 For questions, please contact us at [submissions@jove.com](mailto:submissions@jove.com) or +1.617.945.9051.



# Signature Certificate

Document Ref.: QUMRB-DH5AA-6D5BM-FJ8B4

Document signed by:

	<p><b>Naglaa Shoukry</b> Verified E-mail: naglaa.shoukry@umontreal.ca</p> <p>IP: 206.167.168.130      Date: 30 Aug 2019 20:41:22 UTC</p>	<p><i>Naglaa Shoukry</i></p> 
---	--	--

Document completed by all parties on:  
30 Aug 2019 20:41:22 UTC

Page 1 of 1



Signed with PandaDoc.com

PandaDoc is the document platform that boosts your company's revenue by accelerating the way it transacts.

